STRENGTHENING RECTANGULAR BEAMS WITH NSM STEEL BARS AND
EXTERNALLY BONDED GFRP

by

AUGUSTINE F. WUERTZ

B.S., Kansas State University, 2011

A THESIS

submitted in partial fulfillment of the requirements for the degree

MASTER OF SCIENCE

Department of Civil Engineering
College of Engineering

KANSAS STATE UNIVERSITY
Manhattan, Kansas

2013

Approved by:

Major Professor
Dr. Hayder Rasheed

Abstract

The technology of FRP strengthening has matured to a great extent. However, there is always room for performance improvements. In this study, external bonding of GFRP and near surface mounting (NSM) of regular steel bars is combined to improve the behavior, delay the failure, and enhance the economy of the strengthening. E-Glass FRP is selected due to its inexpensive cost and non-conductive properties to shield the NSM steel bars from corrosion. On the other hand, the use of NSM bars gives redundancy against vandalism and environmental deterioration of the GFRP. An experimental program is conducted in which four rectangular cross-section beams are designed, built, and tested in four-point bending. The first beam is tested as a control beam failing at about 12.24 kips. The second beam is strengthened using two #5 steel NSM bars and 1 layer of GFRP, both extending to the support. This beam failed at 31.6 kips. The third beam is strengthened with the same system used for the second beam. However, the NSM steel bars were cut short covering 26% of the shear-span only while the GFRP was extended to the support. This beam failed at 30.7 kips due to reaching the full flexural capacity of the section at the NSM bars cut off point and the shear stress concentration at the steel bar cut off point. The fourth beam was strengthened with same system as the third beam but then submerged in a highly concentrated saline solution for six months and then tested. This beam failed at a maximum applied load of 29.8 kips, which shows that the GFRP sheet provided good corrosion resistance from the saline solution.

Table of Contents

List of Figures

List of Tables

Acknowledgements

Dedication

      I would like to dedicate this thesis to my wife, Whitni, who helped support me through the whole process and throughout all the years we have been together. I would also like to dedicate this thesis to my parents, family, friends, and colleagues. Without you, I would not be where I am today. Thank you all very much.

Chapter 1 - Introduction

Background

In 2013, the American Society of Civil Engineers (ASCE) published a report card on the state of the national infrastructure. The overall grade of the nation's infrastructure was given a grade of D+, with roads receiving a D, schools a D, and bridges a grade of C+. As of December 2013, one out of nine bridges was categorized as structurally deficient, while the average age of the nation's 607,380 bridges is currently 42 years (ASCE, 2013). Therefore the needs to upgrade, repair, or replace these structures or their structural elements are ever increasing with every year and the increase in population. Retrofitting or repairing structures has become a very efficient and cost effective solution to older, degrading structures or structural elements. Many have found that using steel beams or increasing the section size can be effective ways to increase the flexural and shear capacity of concrete structural elements such as beams or girders. However these methods of strengthening concrete elements involve heavy equipment and many man hours to incorporate. Therefore, considerable research has been performed on using externally bonded fiber reinforced polymers (FRP) due to their light-weight, ease of installment, and high strength-to-weight ratio. Many studies were conducted on rectangular beams retrofitted with externally bonded carbon fiber reinforced polymer (CFRP) and/or glass fiber reinforced polymer (GFRP) fabric sheets or textiles. The results of these studies show that using externally bonded FRP can increase the flexural capacity, slightly the stiffness, and durability of concrete structural elements. However, there is always room for further improvements in this method of strengthening.

In the past ten years, the strengthening technique of near surface mounted (NSM) reinforcement has received more attention as an alternative for externally bonded FRP laminates and plates in the flexural strengthening of concrete elements. The idea of NSM reinforcement started in Europe by using steel rebar between 1940 and 1950. The NSM technique involves cutting into the cover concrete on a structural element and bonding reinforcement using a strong adhesive. The reinforcement may include steel rebars, as well as the new technique of utilizing FRP bars or tapes due to their corrosion resistant properties. The advantages of using NSM reinforcement over externally bonded reinforcement is that the concrete cover and adhesive provide protection

against vandalism and mechanical damage. Also, the NSM technique can delay the debonding of the reinforcement, compared to externally bonded reinforcement.

Therefore, using NSM reinforcement can increase the flexural capacity and stiffness more than using externally bonded reinforcement. The corrosion of steel in reinforced concrete structures and elements is a major problem in the United States and throughout the world, costing billions of dollars in needed repairs and damages. Therefore, the use of externally bonded FRP and NSM reinforcement to not only strengthen and repair but to also help prevent further corrosion in concrete structures are very desirable methods. Externally bonded FRP sheets can provide resistance from deicing salts, chemicals, and environmental erosion. GFRP sheets have better corrosion resistance qualities as well as non-conductive properties as compared to CFRP sheets. However, further long-term research is needed to fully understand the corrosion resistive properties of all types of FRP.

Objectives

The main objective of this research project is to determine the flexural behavior of rectangular concrete beams that are retrofitted with NSM steel rebar and also externally wrapped with a GFRP sheet secured with GFRP U-wraps. By combining these two techniques, the lifespan of concrete beams, girders, or other elements could be lengthened greatly. Also this could be a less costly approach to strengthening than other techniques, especially those that use only externally bonded FRP systems. To achieve this objective, the secondary objective of comparing the effects of shortened NSM steel rebars versus full length NSM steel rebars was also performed. Another main objective of this research is to study the effects of an accelerated corrosion bath will have on the bond and overall strength of the beams. Many concrete elements are exposed to weathering processes as well as many man-made chemicals that corrode and weaken the concrete and internal reinforcement. To achieve this goal, one beam was submerged in a highly concentrated salt bath for six months and then tested to failure in order to compare to the other strengthened beams.

Complete design and construction details of the beam specimens will be discussed in this thesis along with test methods and experimental setup and procedures. Finally, conclusions and recommendations for future research will be discussed.

Scope

This thesis is broken up into seven main chapters, with the first chapter being an introduction. Following the introduction will be a literature review in which the following three main topics are reviewed: externally bonded FRP, near surface mounted bars, and corrosion of steel bars. Following that will be a discussion of the design and construction of the specimens. This section will include discussions on design, construction of formwork and caging, casting, and the strengthening procedure. Next will be discussion of the material properties of the concrete, GFRP, and steel used to construct and strengthen the specimens. The setup and testing procedures of each of the beams will be discussed next followed by the results of the testing. The results are then analyzed and compared to theoretical values. Finally, the last section will consist of conclusions from this research and recommendations for future work.

Chapter 2 - Literature Review

Overview

Research has shown that using externally bonded FRP sheets or using near surface mounted steel or FRP bars can greatly increase the flexural capacity of the concrete specimens. Traditionally, these two techniques of strengthening beams have not been utilized together, however many experiments have been performed using either one of these techniques to increase the flexural capacity of concrete beams.

A large problem of using NSM steel bars or even internal steel reinforcement is that once it is exposed to the environment, the steel will oxidize and rust, thus decreasing the tension capacity of the steel and the moment capacity of the beam.

This section will have three main parts that relate to the research reported in this thesis. First, a review of literature will be done on the effect of externally bonded FRP on reinforced concrete beams. Second, the literature review will discuss the effect of near surface mounted bars will have on the flexural capacity and ductility of reinforced concrete beams. Finally, the last section of the literature review will pertain to the research already performed on the corrosion of steel in reinforced concrete beams.

Externally Bonded FRP

In 1997, Arduini and Nanni performed an experiment in which they studied the behavior of reinforced concrete beams that were pre-cracked and then strengthened with CFRP sheets. The beams in this experiment were divided into two series (S and M), a set of 9 beams with a shorter length and another set of 9 beams with a longer length. The S-series beams had a length of 1500 mm with a height of 160 mm and width of 320 mm. The M-series beams had a length of 2100 mm with a height of 320 mm and a width of 160 mm. The internal reinforcement for the S and M beams are 4-12 mm and 4-16 mm diameter steel rebars, respectively. A number of the beams were then preloaded (pre-cracked) prior to the application of the FRP sheets, while the rest remained un-cracked prior to strengthening. Two different types of pre-impregnated CFRP sheets were used (M and T), one with a modulus of 235 GPa and the other with a modulus of 380

GPa. Not only was the type and amount of external FRP varied but the surface preparation techniques were varied between basic sanding and sandblasting of the concrete surface. The results of the four-point bending tests showed that in all of the different cases, the pre-cracked beams strengthened showed very similar results in ultimate moment capacity and deflection to the un-cracked beams that were also strengthened with the same external reinforcement. Many of the beams showed significant improvement in moment capacity over the control beams; with the highest reaching approximately 200% greater or two times the capacity. The majority of the failure modes included debonding of the FRP sheet, which creates a very brittle behavior, while the beams anchored with U-wraps achieved higher capacities and failure modes of rupturing of FRP. This study showed that repairing in-service beams is easy and produces results similar to those of virgin beams. Also, the use of U-wrapping helps to prevent debonding of FRP sheets which results in a higher moment capacity. Also, the effectiveness of FRP strengthening is a function of the beam shape and amount of steel reinforcement.

Kachlakev and McCurry (2000) performed a study of four full-scale RC beams that were replicated from an existing bridge and strengthened the beams with flexural and shear externally bonded FRP. The beams had the dimensions of 6096 mm long, 305 mm wide and 762 mm deep. The beams were constructed without steel stirrups, which is the case on the existing bridge, therefore shear failure of the beams are a major concern. CFRP unidirectional sheets were used to increase flexural capacity and GFRP unidirectional sheets were used as the shear reinforcement. One beam was left un-strengthened to use as a control beam. One beam was strengthened only with the CFRP for flexure, one beam was strengthened with the GFRP for shear only, and the last beam was strengthened with both for flexure and shear. The beams were tested in four point bending. The control beam and the beam reinforced with the CFRP sheets for flexure only both failed in shear with diagonal tension cracks forming. The beam strengthened with the GFRP sheets for shear only failed with a ductile crushing of concrete failure mode. This showed that the external shear reinforcements were enough to replace the missing internal steel stirrups. The beam strengthened for both flexure and shear did not fail, since its capacity exceeded that of the loading machine. However, it is believed to have a failure mode of yielding of tension steel followed by crushing of concrete or ductile concrete crushing. Both the flexure only and shear only strengthened beams had an increase in load capacity of 145% over the

control beam. The beam strengthened for both shear and flexure is believed to have an increase in load capacity of over 152%. This beam had a 200% increase in the maximum applied moment over the control beam.

Rahimi and Hutchinson (2001) conducted research on strengthening concrete beams with externally bonded FRP plates. Thirty one (31) beams were constructed with dimensions of 200 mm wide x 150 mm deep x 2300 mm long. The beams were broken up into three different types (A-C), where types A and B have steel reinforcement ratios of 0.65% and type C has a steel reinforcement ratio of 1.68%. Also, Beams A8 and A9 were pre-loaded to crack the beams and were then strengthened to represent cracked beams in service that need to be strengthened or repaired. The external reinforcements include CFRP and GFRP unidirectional fiber plates, having fiber volume contents of 40% and 50%, respectively as well as externally bonded steel plates. The plates consisted of thickness ranging from 0.4 to 1.2 mm for the CFRP and 1.8 mm for the GFRP, due to its relatively low modulus. The beams were strengthened using basic surface preparation and curing procedures. The beams were tested in four-point bending, with a clear span of 2100 mm, with the load being applied in increments of 5 kN. The failure modes of the strengthened beams ranged from ductile concrete crushing to cover delamination to concrete shear failure followed by cover delamination. All of the strengthened beams performed significantly better than the control beams, in terms of strength and stiffness. Typically, the strengthened beams had a twofold increase in flexural capacity with the highest being approximately 230% stronger than the respective control beam. Also, it was seen in the results that a beam strengthened with only two plies of CFRP plating will have a similar flexural capacity of a beam containing a much higher percentage of conventional reinforcement. The beams strengthened with the steel plates were stronger in the Type B beams while they were much weaker than the FRP equivalents in Type C beams. From this experiment, it can be concluded that using externally bonded FRP can greatly increase the flexural capacity of reinforced concrete beams. Also, the magnitude of performance increase is influenced by the composition of the concrete beams and also by the type and amount of external reinforcement.

Nurbaiah et al (2010) did a research experiment on the comparison of externally bonded FRP sheets and NSM FRP rods. The experiment was strengthening four RC beams, one beam with

one NSM GFRP rod, one beam with two GFRP rods, one beam with one ply of CFRP fabric, and finally one beam with two plies of CFRP fabrics. One beam was left un-strengthened in order to be a control beam. The beams were 2325 mm long with a width of 170 mm and a depth of 270 mm. The beams were tested in four point bending. The test results showed that the beams strengthened with one and two GFRP rods had an increase in capacity over the control by 40% and 88%, respectively. The beams strengthened with one and two plies of CFRP fabric had an increase in load capacity over the control by 8% and 16%, respectively. The beams strengthened with the CFRP fabrics failed by the de-bonding of the fabric sheets and the beams strengthened with NSM GFRP rods failed in a ductile crushing concrete mode. The stiffness increase over the control ranged from 26% to 85%, with the beams strengthened with the NSM rods being the highest of the four strengthened beams.

Near Surface Mounted Bars

Hassan and Rizkalla (2004) conducted a study to investigate the bond characteristics of NSM CFRP bars. Eight concrete beams with spans of 2.5 m and depths of 300 mm were constructed with two 10-mm diameter bars are used for tensile steel. Four beams were strengthened with NSM CFRP bars with embedment lengths of 150, 550, 800, and 1200 mm using a gel epoxy adhesive mainly used for structural repairs. Three beams were strengthened with NSM CFRP bars with embedment lengths of 550, 800, and 1200 mm using an epoxy adhesive mainly used for grouting bolts, dowels, and steel bars in concrete. The beams were tested using a concentrated load applied at mid-span. The un-strengthened control beam failed at an ultimate load of 56 kN with a failure mode of ductile concrete crushing. All strengthened beams failed when the NSM CFRP bars debonded, with the ultimate load applied ranging from 56 to 79 kN. The failure load and overall efficiency of the bar strength increased with the increasing of the embedment length. From the results of this study, it can be concluded that the use of NSM CFRP bars is an effective way to strengthen or repair concrete beams and structures. Also, the development length of NSM FRP reinforcement is highly dependent on the dimensions of the bars, concrete and adhesive properties, reinforcement configuration, and groove width and the behavior of NSM FRP bars will behave much differently than that of NSM steel bars.

Soliman et al (2010) executed a study on the flexural behavior of concrete beams strengthened with NSM-FRP bars. A total of 20 reinforced concrete beams were tested. The beams were separated into three different series (A-C), with the internal reinforcement ratio increasing with each series (0.4%, 0.8%, and 1.6%). The beams all had dimensions of 200 mm in width, 300 mm in depth, and 3010 mm in length. Also the bonded length of the NSM bars was increased within each series, as well as the type of NSM bars being changed between carbon and glass FRP. The CFRP bars used had two different diameters, 9.5 and 12.7 mm, while the GFRP bars had a diameter of 12.7 mm. Only a single groove was cut into each of the beams in order to strengthen them with the NSM bars. The beams were tested in four-point bending over a simply-supported span of 2.6 m, until failure at a rate of 1.2 mm/min. All of the strengthened beams had a failure mode of cover delamination, starting at the cut-off points of the NSM-FRP bars. From the results, several things can be concluded. One conclusion is that using the NSM-FRP bars is an efficient way to increase the flexural capacity and stiffness of concrete beams. The increase of bond length will result in an increase in capacity, up to a limit of approximately 48 times the bars diameter. The NSM-FRP bars system was more effective with beams with low reinforcement ratios. Also, the GFRP bars showed similar increases in the beams' carrying capacities to those of CFRP bars. In the beams with a steel reinforcement ratio of 0.4%, the strengthened beams showed an increase in total applied load capacity over the control beam ranging from 22 to 104%.

Zhang et al (2011) performed research on the flexural behavior and ductility of reinforced concrete beams with NSM GFRP bars. Seven beams were tested, with two being used for control beams and five beams being strengthened. The beams had a rectangular cross section with spans of 2.2 m, widths of 150 mm, and depths of 300 mm. The beams were internally reinforced with compression steel and tension steel composed of two steel bars with diameters of 8 mm and 12 or 14 mm, respectively. The main parameters in this experiment were the steel reinforcement ratio, ρ, and the number of NSM GFRP bars. The GFRP bars had nominal diameters of 7.9 mm and 10 mm. Beams BA0, BA1, BA2, and BA3 had a $\rho = 0.6$ while beams BB0, BB1, and BB2 had a $\rho = 0.81$. All of the beams were tested in four point bending. Beams BA0 and BB0 were the control beams and failed in flexure at loads of 65.4 kN and 68.9 kN, respectively. Beams BA1 and BB2 were strengthened with one 7.9 mm diameter GFRP bar and had ultimate loads of

86.5 kN and 104.5 kN, respectively. Beams BA3 and BB1 were strengthened with one NSM GFRP bar with diameter of 10 mm. These beams failed at an ultimate load of 95.5 kN and 105.5 kN, respectively. Beam BA2 was strengthened with two 7.9 mm diameter NSM GFRP bars. Beam BA2 failed at an ultimate load of 109.8 kN. All strengthened beams had a failure mode of rupture of the NSM GFRP bars. The GFRP bars did not de-bond but were utilized to their full capacity. For specimens BA1 to BA3, the increase in the flexural capacity over the control beam BA0 ranged from 32% to 68%. For specimens BB1 and BB2, the increase in flexural capacity over the control beam BB0 was 53% and 52%, respectively.

A similar study was done by Sun et al (2011) in which a steel fiber reinforced polymer composite bar (SFCB) was used as NSM reinforcement for strengthening concrete beams. A SFCB is a bar in which regular steel bars are wrapped, using a pultrusion process, with a FRP skin made up of different types of fibers. Seven beams were cast including one un-strengthened control beam, one beam strengthened with NSM ordinary steel bars with diameter 14 mm, four beams strengthened by NSM SFCBs, and one beam strengthened with two CFRP bars with a diameter of 8 mm. The beams were 2.0 m long with a width of 150 mm and a depth of 300 mm. Two NSM grooves were chiseled into the soffit of the beams with a length of 1700 mm centered on the beam. The beams were tested in four point bending. The control beam failed at a maximum load of 163.6 kN in a ductile crushing of concrete failure mode. Beams B-B20 and B-B30 were strengthened with NSM SFCBs in which the FRP type used was basalt FRP (BFRP). These two beams failed at an ultimate load of 269.6 kN and 284.6 kN, respectively. This is an increase in the ultimate load capacity over the control by 65% and 74%, respectively. Beam B-B20 failed by tensile steel yielding and the SFCB outer FRP rupturing, which resulted in concrete crushing. Beam B-B30 failed by the tensile steel yielding and the SFCBs de-bonding. Beams B-C24 and B-C40 were strengthened with SFCBs in which the outer FRP was carbon FRP. These beams failed with ultimate loads of 259.3 kN and 283.5 kN, respectively. This is an increase in the ultimate load capacity over the control by 58% and 73%, respectively. Beam B-C24 failed in a similar mode as B-B20 and beam B-C40 failed in a similar de-bonding mode as beam B-B30. Beam B-CF8 was strengthened with CFRP bars and Beam B-S14 was strengthened with steel only. These two beams failed at an ultimate load of 260.9 kN and 288.8 kN, respectively. This is an increase in the ultimate load capacity over the control by 59% and 76%,

respectively. Beam B-CF8 failed in a de-bonding failure mode which was followed by yielding of the tensile steel. Beam B-S14 had a ductile concrete crushing failure mode, similar to the control beam. This experiment shows that using NSM steel bars and SFCBs can greatly increase the capacity of a beam.

Corrosion of Steel Bars in RC and Bond Behavior of FRP

Soudki et al (2000) conducted an experimental study to investigate the viability of using externally bonded FRP laminates to rehabilitate corrosion-damaged RC beams. Sixteen small scale and twenty larger scale beams were constructed with variable chloride levels from 0 to 3%. The beams were then repaired by externally epoxy bonding FRP laminates to the concrete surface. The tensile reinforcement was then subjected to accelerated corrosion by the means of a current impressed through it. Following the corrosion process, the beams were tested in flexure in a four-point bending setup. The test results showed that the FRP laminates successfully confined the corrosion cracking and spalling due to expansion of corrosion products. The FRP also successfully increased the stiffness, ultimate strength, and yield strength over un-strengthened specimens. From this study, it can be concluded that the use of FRP sheets for the strengthening of corroded RC beams is an efficient technique that can maintain structural integrity and enhance the behavior of such beams.

Wang et al (2004) performed an experimental study on the behavior of CFRP retrofitted RC beams under static loading, which possess high chloride content and rebar corrosion. Twenty four RC beams with dimensions 20 x 35 x 350 cm were cast and divided into two groups, according to the compressive strength of their concrete. There are many different parameters that were varied in this study including: compressive strength of concrete, accelerated corrosion power, cathodic protection, natural or accelerated corrosion, layers of CFRP strips, epoxy injected cracks, and CFRP U-shaped wraps. Seventeen of the beams were retrofitted using 10 cm wide FRP sheets on the tensile side of the beam and then secured with U-shaped FRP strips 10 cm wide spaced every 20 cm along the sides of the beams. The FRP increases the flexural capacity of the beams and also helps to prevent separation of the concrete due to corrosion as well as providing additional corrosion protection. The majority of the beams had a failure mode of tension steel yielding and breaking of FRP strips. From the results, it was concluded that the

beams strengthened with FRP strips increased over that of the un-strengthened beams. It can also be concluded that the use of CFRP as corrosion protection and flexural strengthening is viable and efficient. Finally, it can be shown that the beams constructed with high chloride content and exposed to high corrosion environments perform not as well as their counterparts, but can be strengthened to a level that will be comparable to them by using CFRP sheets and U-shaped wraps.

Soudki et al (2007) also performed a study in which beams strengthened with CFRP sheets and strips were subjected to an aggressive saline environment. Eleven beams were constructed, with eight being cracked and three remaining un-cracked to act as control. The beams were 150 mm wide by 250 mm deep by 2.4 m long and lightly reinforced with a reinforcement ratio of 0.6%. CFRP sheets and strips were used to strengthen the cracked beams. The sheets had an ultimate strength of 3480 MPa and modulus of 230 GPa while the strips had an ultimate strength of 2800 MPa and modulus of 165 GPa, both which are based on the dry fiber properties. In terms of environmental exposure, three beams were kept in a normal lab environment while the other eight were subjected to wetting and drying cycles (100, 200, and 300 cycles) in the presence of deicing chemicals (3% NaCl) at room temperature. The wet-dry cycle took 2 days to complete, which consisted of 1 day of wetting followed by 1 day of drying. Following the environmental exposure, two non-destructive tests were performed on the beams: electrical potential measurements and corrosion rate measurements. The specimens were then tested monotonically until failure in a four point bending procedure. From the non-destructive tests, it was shown that the beams that underwent 0 or 100 cycles had zero or negligible amounts of mass loss in the steel. However, beams that underwent 200 or 300 cycles had mass losses of 1.0% and 1.3%, respectively. All un-strengthened beams failed by steel yielding while all other beams except the beam strengthened with CFRP strips undergoing 0 cycles failed in debonding of the CFRP. Beam S-0 failed by rupture of the CFRP strips. The un-strengthened beams failed at ultimate moments ranging from 23.83 kN-m to 25.36 kN-m. The beams strengthened with the CFRP strips had ultimate moment capacities ranging from 44.17 kN-m to 31.91 kN-m, with the ultimate moments decreasing with the increase in number of wet-dry cycles. The beams strengthened with CFRP sheets performed better than the beams strengthened with CFRP strips, with the ultimate moments ranging from 48.46 kN-m to 43.31 kN-m, with the ultimate moments

decreasing with the increasing number of wet-dry cycles. From this study it can be concluded that CFRP sheets and resin system appeared to decrease the chloride ionic diffusion and may reduce the corrosion rate of the reinforcing steel. Also, the load capacity was enhanced with the CFRP sheets and strips to almost double that of the un-strengthened beams. Finally, the ultimate capacity of the CFRP strengthened beams decreased by 11 to 28% over 300 cycles while the stiffness and yield load were not affected.

Dai et al (2010) performed research on the bond behavior of FRP to concrete interfaces with the influence of moisture. Two types of tests were conducted, bending tests and pull-off bond tests, to evaluate the shear and tensile bond performance of FRP-to-concrete interfaces. Fifty six (56) specimens were constructed and tested, 48 of which were plain concrete beams strengthened with FRP sheets bonded to the soffit of the beams. The other eight specimens were prepared for the tensile pull-off bond tests. All of the concrete used had a water-to-cement ratio of 0.5 and a fine-to-coarse aggregate ratio of 0.49. The beams were strengthened with a new carbon FRP sheet, formed from 1.0 to 2.0 mm diameter carbon fiber strands, called carbon strand sheet. The test variables included concrete substrate moisture content at the time of FRP bonding, relative humidity of the air during FRP composite curing(40 and 90%), adhesive primer type(normal and hydrophobic), bonding adhesive type(normal and ductile), and exposure duration(not exposed, 8 months, 14 months, and 2 years). From the results of this experiment, several conclusions were made. Different values of the relative humidity in the air during curing, with values up to 90%, had very little effect on the bond performance of the FRP. Surface moisture at the time of installation can greatly affect the bond performance of the FRP, resulting in premature debonding of FRP during loading. However, this can be eliminated if a hydrophobic type primer is used. Also, the flexural capacity and corresponding maximum deflection generally decreased with the increase in exposure time.

Chapter 3 - Design and Construction of Specimens

Design of Rectangular Beams

The design of the four beams was performed based on ACI 318-11 with strain compatibility and force equilibrium. The geometry was chosen so that the beam would fail in flexure. The external flexural reinforcement was designed based on ACI 440.2R-08 using the same principles.

Additional shear reinforcement was unnecessary. However, U-wrap anchorage external stirrups were used in order to prevent delamination of the concrete cover or debonding of the GFRP sheet. The U-wrap stirrups were designed based on the shear friction model of ACI 318-11 adapted by Rasheed et al. (2006) to provide continuous anchorage to the GFRP and NSM bars. The tension force in the stirrups is determined by clamping a horizontal crack through shear friction. The horizontal shear per unit length of the plated shear span can be found from maximum tensile force divided by the shear span. The area of anchorage reinforcement needed can then be found by equating the tension in the U-wraps per unit length to the area of these stirrups multiplied by their allowable stress. Accordingly and based on the properties of the GFRP sheets, the spacing can then be calculated. The size of the GFRP stirrups was determined to be 8.5 inches wide and spaced every 1 foot on center applied as a single layer. An additional double anchorage of 20.5 inches wide U-wrap is applied, 10.25 inches on both sides of the short NSM bars cut off points in beams R4 and R5. Below are the calculations of the U-wrap anchorage.

At the ultimate analytical flexural load of 30.8 kips, the maximum tension force in the NSM bars and GFRP is:

$$T_{NSM} = 43.4 \text{ k} \tag{1}$$

$$T_{GFRP} = 25.5 \text{ k} \tag{2}$$

$$T_{total} = 68.9 \text{ k} \tag{3}$$

$$V_{hu} = \frac{68.9 \text{ k}}{5.5 \text{ ft}} = 12.53 \frac{\text{k}}{\text{ft}} \tag{4}$$

$$T_{sf} = \frac{V_{hu}}{\mu} = \frac{12.53 \text{ k/ft}}{1.4} = 8.95 \text{ k/ft} \tag{5}$$

$$T_{sf} = \emptyset\, A_{vf} E_f \varepsilon_{fe} \tag{6}$$

$$8.95\frac{k}{ft} = 0.75\, A_{vf} * 3790\ ksi * 0.00375 \tag{7}$$

$$A_{vf} = 0.84\ in^2/ft \tag{8}$$

$$A_{vf} S = 2nt_f\, w_f \tag{9}$$

$$0.84\frac{in^2}{ft} * 1ft = 2 * 1 * 0.05in\ w_f \tag{10}$$

$$w_f = 8.4\ in \approx 8.5\ in\ \text{for every 1 ft on center} \tag{11}$$

Where:
$T_{total} = T_{NSM} + T_{GFRP}$
V_{hu} = shear force per unit length of shear span
T_{sf} = shear friction
μ = coefficient of friction
ϕ = strength reduction factor
A_{vf} = area of FRP shear reinforcement
E_f = Modulus of Elasticity of FRP
ε_{fe} = effective strain in FRP
n = number of layers of FRP
t_f = thickness of FRP U-wraps
w_f = width of FRP shear U-wraps

Beam Geometry

The laboratory testing equipment that is used to test the beams has an actuator capacity of 50 kips. Therefore it is important that the maximum load capacity of the strengthened beams not exceed the 50 kip limit of the actuator. The design was performed using a flexural analysis program developed by a former graduate student at Kansas State University. The dimensions that allowed a flexural failure mode and fell below the 50 kip limit were used. The beams have a rectangular cross section with a width of 6 in. and height of 12 in. The length of each beam was 16 ft. long with a clear span of 15.5 ft. The main flexural reinforcement consists of 2 No. 5 bars with 2 No. 3 bars used for compression steel and to help form the cages. The shear reinforcement consists of No. 3 stirrups spaced 5 inches, center to center. Figure 1 below shows the cross section dimensions of all the beams. Figure 2 shows the reinforcement details of the control beam (Specimen R1) and Figure 3 shows the reinforcement for the beams strengthened with 2 full length No. 5 NSM steel rebars and an externally bonded GFRP sheet (Specimen R2). Figure 4 shows the reinforcement details for the beams reinforced with 2-7.0 ft. long No. 5 NSM steel rebars and an externally bonded GFRP fabric sheet (Specimens R3 and R4).
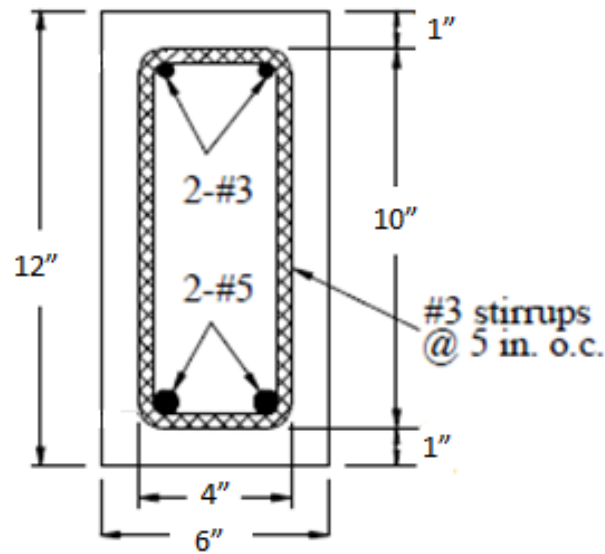
Figure 1: Beam Dimensions
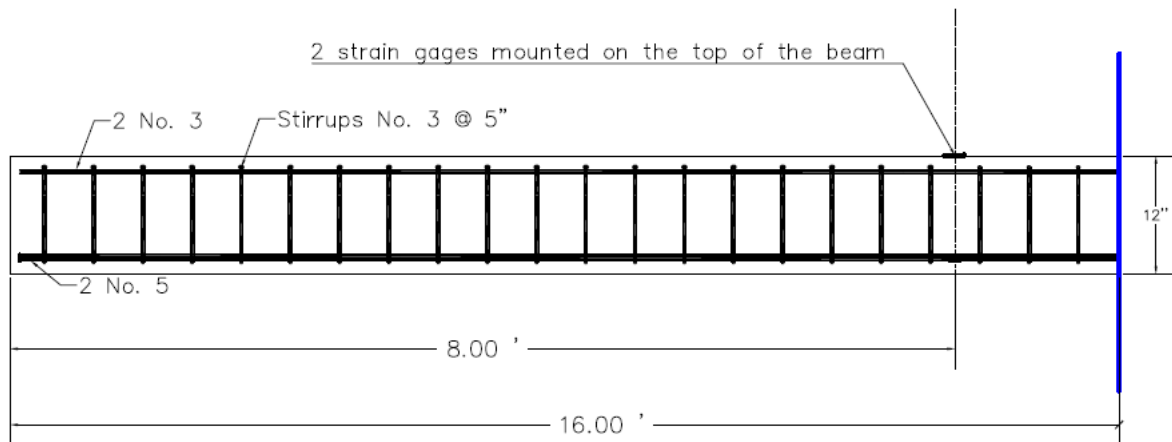
Figure 2: Reinforcement Details for the Control Beam
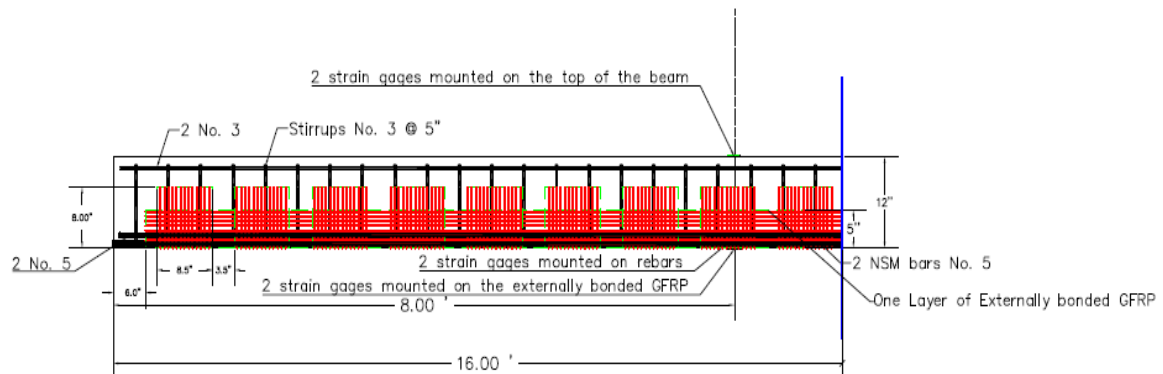
Figure 3: Reinforcement Details for Full Length NSM rebars Beam (Specimen R2)
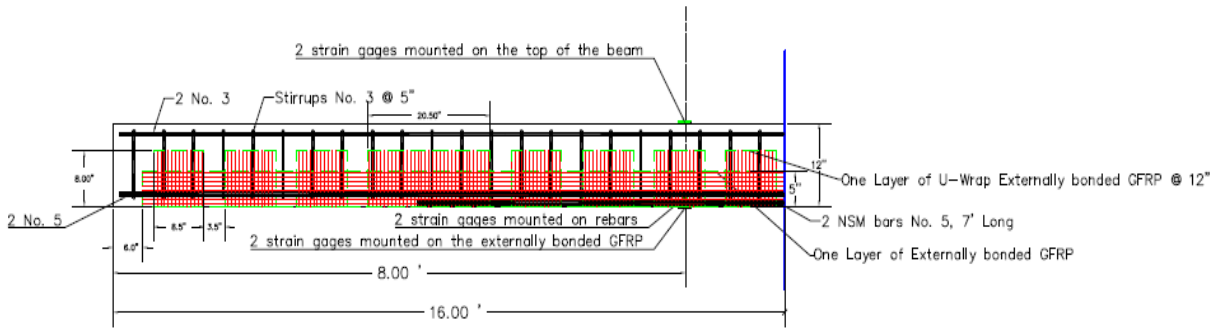
Figure 4: Reinforcement Details for 7.0 ft. NSM rebars Beams (Specimens R3 & R4)

Formwork and Steel Caging

The formwork consisted of plywood sheets and 2 in. x 4 in. lumber boards. All beam specimens were constructed onsite at the Civil Engineering wood and steel workshops. The plywood sheets were 4 ft. x 8 ft.; therefore two sections of the formwork were constructed and then attached to each other outside in the area of casting, in order to create the 16 ft. long specimens. Wooden rods of 1 in. x 1 in. were cut and screwed into the bottom of the formwork to create grooves for the NSM bars when casting. These wooden rods were chiseled out after the beams were finished curing. All four specimens were able to fit into one set of formwork. Figure 5 below shows the formwork for the four beam specimens.

16

Figure 5: Formwork for the Beam Specimens

The steel used for reinforcement was donated by Ambassador Steel Inc., a company based out of Kansas City, MO. The steel rebars used for longitudinal reinforcement were cut to appropriate length in the steel shop using a steel chop/rotating saw. The steel rebars used for stirrups were cut to length in the same fashion and bent to the correct dimensions using a manual bending machine in the steel shop. The longitudinal steel and the stirrups were fastened together using rebar ties. Figure 6 below shows the finished rebar caging used for the four beams. Two strain gages were mounted on the bottom steel reinforcement at the mid-span of the beam, as shown in Figure 7. One inch steel chairs were used in the formwork to lift the beam to allow for concrete cover on all sides of the beams. Figure 8 shows the steel caging in the formwork, ready before casting. The strain gage wires were protected by running the wires through plastic tubing and the gage itself was protected by taping around it. Steel rebar hooks were made and placed at the third points of the beams in order to lift and manipulate the beams once cast.

Figure 6: Steel Rebar Caging used for Beams
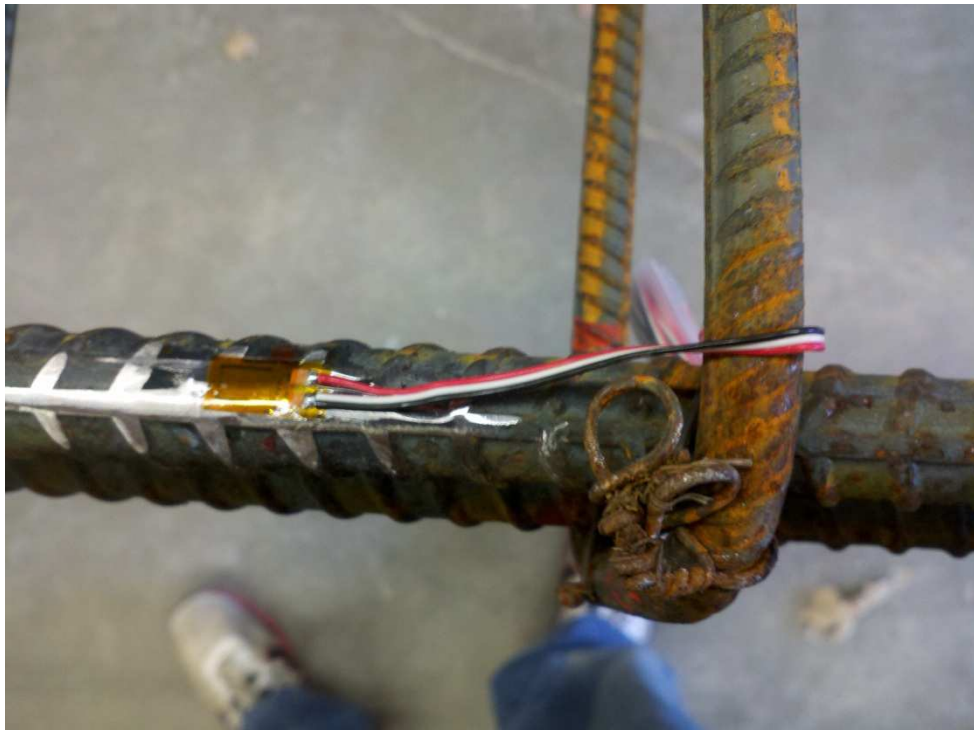
Figure 7: Strain gage attached to Steel Reinforcement

Figure 8: Steel Caging in Formwork before Casting

Casting of Specimens

The specimens were cast using 8000 psi ready mix concrete provided by Midwest Concrete Materials, a local provider. A number of undergraduate and graduate students, along with faculty assisted with the casting of the specimens. Along with the beams, cylinders were cast in order to conduct compressive strength test on. The beams and cylinders were allowed to cure for 28 days. The beams were covered in an insulating concrete blanket since the temperature outside was cold and loss of heat and moisture would prevent proper curing. Several cylinders were left outside to cure with the beams and the rest were placed in a moisture room to cure. Figure 9 and Figure 10 show the casting of the specimens. Figure 11 shows the casting of concrete cylinders and Figure 12 shows the concrete blanket used to cover the beams to allow for proper curing. After the beams were fully cured, steel bars were epoxied into the ends of the beam to use when flipping the beam to apply the GFRP sheets and stirrups.

Figure 9: Casting of the Specimens

Figure 10: Casting of the Specimens

Figure 11: Casting of Concrete Cylinders

Figure 12: Covering Specimens with Concrete Blanket

Installation of NSM Bars

The first step in strengthening the beams was to install the NSM steel rebars into the grooves. The wooden rods were chiseled out of the grooves, which can be seen in Figure 13, and then the grooves were sandblasted using a portable sandblaster attached to an air compressor. Sandblasting the grooves helps to remove any remaining wood particles or other undesirable debris which could affect the bond of the epoxy to the concrete. It also roughens the surface which also helps with the bonding process. After sandblasting, the grooves were blow out using an air compressor. Epoxy was mixed according to the manufacturers specifications, which was mixing the two part resin and then adding silica fume until the mixture had a thick, almost peanut buttery texture. To install the NSM bars, the grooves were filled slightly more than halfway full, and then the bars were pushed into the grooves so that they were sufficiently surrounded by epoxy. Excess epoxy was then scraped off using putty knives until the epoxy was flush with the soffit of the beam as seen in Figure 14. Once finished, the epoxy was allowed to sit for 24 to 36 hours to ensure proper curing and bonding. Figure 15 shows the beams after the NSM bars have been completely installed.

Figure 13: Chiseling out Wooden Pieces

Figure 14: Scraping off Excess Epoxy during Installation of NSM bars

Figure 15: Beams with NSM bars Installed

Surface Preparation

Prior to applying the GFRP sheets and external U-wraps, the surface of the beam was sandblasted in order to roughen the surface and as well as remove any undesirable particles on the concrete, which can be seen in Figure 16. Figure 17 shows the difference between a sandblasted surface and a non-sandblasted surface. After sandblasting, the bottom corners of the beams were rounded off to approximately a 0.5 inch radius, as per ACI 440.2R-08. Rounding the corners not only protects the fibers in the FRP but also helps avoid any stress concentrations at the corners. Figure 18 shows the rounded corners after grinding. After sandblasting and grinding, any large voids or bug-holes were filled with epoxy to create an even surface to apply the GFRP sheets.

Figure 16: Sandblasting the Surface of the Beams

Figure 17: Comparison of Sandblasted (top) vs. Non-Sandblasted (bottom) Surfaces

Figure 18: Rounded Corners from Grinding

Application of GFRP

Once the surface preparation was complete, it was time to apply the GFRP sheets and U-wraps. The beams were taken inside so that the epoxy and GFRP system would not be affected by moisture or extreme temperatures from the weather. Once inside the beams were flipped so that the soffit was facing upwards. Resin was mixed according to the manufacturer and then applied to the surface. The GFRP sheets were then placed onto the surface. The GFRP sheet was pressed into the resin using wooden and plastic rollers. By doing this, any air pockets or voids were eliminated, thus creating a better bond. More resin was then applied to the GFRP sheet to ensure that the fibers would be completely saturated. Next the GFRP U-wraps were placed onto the GFRP sheet, at 1 foot intervals, with their fibers running in the transverse direction of the beam, which can be seen in Figure 19. These were also rolled flat onto the surface with rollers to avoid any air pockets as seen in Figure 20. Additional resin was also applied onto the U-wraps to fully saturate the fibers. Figure 21 shows the fully strengthened beam after the application of the GFRP is complete.

Figure 19: Applying U-Wraps

Figure 20: Removing Air Pockets by Rolling U-Wraps

Figure 21: Finished Fully Strengthened Beam

Chapter 4 - Material Properties

Testing of Concrete Cylinders

The concrete used in casting the beam specimens was a ready mix concrete with a nominal compressive strength of 8000 psi. While casting the beams on 1/24/12, twenty-two 4 in. x 8 in. cylinders were poured in order to obtain the actual compressive strength of the concrete. Fourteen of the cylinders were cured in a moisture room and eight were left outdoor with the beams to cure. The first four cylinders were tested on 2/21/12, from which three were taken from the moisture room and one from outside. The average compressive strength of this set was 7941 psi. The second set of four cylinders was tested on 6/22/12 and the average compressive strength of this set was 7995 psi. The third set was tested on 7/5/12 and the average compressive strength of this set was 8484 psi. The fourth set was tested on 11/19/12 and the average compressive strength of this set was 9386 psi. The fifth set of cylinders was tested on 2/13/13 and the average compressive strength of this set was 8759 psi. Table 1 below shows the results of the cylinder tests.

Table 1: Compressive Strength of Concrete Cylinders

CYLINDER	LOAD (lbs)	COMPRESSIVE STRENGTH f'c (psi)	DATE TESTED
C1- outside with no cure	97185	7733	
W1- cured in moisture room	103160	8209	2/21/2012
W2- cured in moisture room	97915	7791	
W3- cured in moisture room	100915	8030	
C2- outside with no cure	95720	7572	
W4- cured in moisture room	104895	8335	6/22/2012
W5- cured in moisture room	105245	8377	
W6- cured in moisture room	102220	7694	
C3- outside with no cure	105246	8376	
W7- cured in moisture room	104896	8344	7/5/2012
W8- cured in moisture room	111546	8873	
W9- cured in moisture room	104880	8342	
C4- outside with no cure	118160	9400	
W10- cured in moisture room	113460	9033	11/19/2012
W11- cured in moisture room	120910	9622	
W12- cured in moisture room	119151	9490	
C5 – outside with no cure	106340	8462	
C6 – outside with no cure	105240	8375	
C7 – outside with no cure	103070	8202	
C8 – outside with no cure	111290	8856	2/13/2013
W13 – cured in moisture room	115815	9216	
W14 – cured in moisture room	118625	9440	

Before casting was started, slump and air content tests were performed on the concrete according to ASTM C143 and ASTM C231, respectively. The slump of the concrete was 2 in. and the air content was tested to be 4.5%. During casting, a vibrator was used to eliminate any air voids in the beams for quality control. Since casting took place on 1/24/12 and the temperature during the night would get below 32°F, an accelerator of Calcium Chloride was added to the concrete. Also, a concrete blanket was used to keep heat and moisture in to allow for proper curing.

Testing of GFRP Coupons

The material properties of the Glass Fiber Reinforced Polymer (GFRP) sheets were given by the manufacturer to be a modulus of 3030 ksi and an ultimate tensile strength of 66720 psi which corresponds to an ultimate strain of 0.022. These sheets were donated by VSL Industries, a composites company based out of Baltimore, Maryland. However, for quality control, a coupon test was also conducted on the GFRP according to ASTM D3039. Figure 22 shows a coupon being tested in tension in a hydraulic load frame. Six 1 in. wide by 10 in. long coupon specimens

were fabricated, as seen in Figure 23, by a wet lay-up process. Three specimens had one layer of GFRP and the other three had two layers of GFRP. After testing all of the specimens, the average modulus was 2168 ksi with an average ultimate strength of 38400 psi corresponding to an average ultimate strain of 0.0177. Table 2 shows the results of the tensile tests performed on the coupons. Appendix A also shows additional data recorded for these tensile tests.

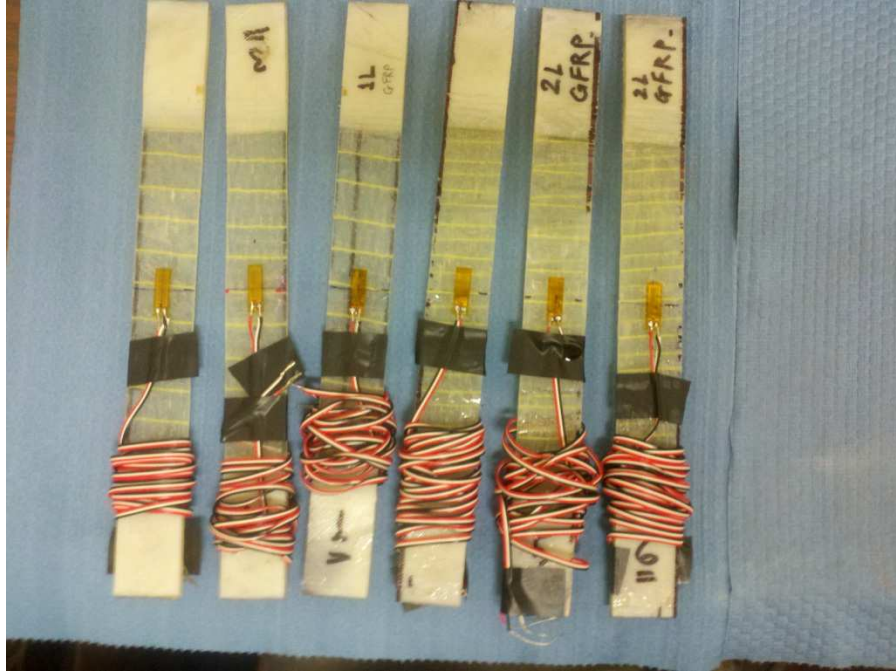**Figure 22: Tensile Test on GFRP Coupon**

Figure 23: Coupon Specimens

Table 2: Results from Coupon Tests

Specimen	Width	Average Thickness	Ultimate Strength (ksi)	Modulus(ksi)	Ultimate Strain (με)
GFRP-1	1.00	0.099	32.7	2173	15065
GFRP-2	1.00	0.103	32.7	1971	16598
GFRP-3	1.00	0.111	31.9	1886	16936
GFRP-4	1.00	0.166	44.5	2026	21954
GFRP-5	1.00	0.142	38.5	2265	16987
GFRP-6	1.00	0.152	50.2	2688	18675
Average GFRP	-	-	38.4	2168	17702

Testing of Steel Bars

The steel used as reinforcement in the beams was donated by Ambassador Steel Inc., a steel provider based out of Kansas City, MO. The tension steel and NSM steel bars were both No. 5 bars (diameter of 0.625 in.) and the compression steel and stirrups were both No. 3 bars (diameter of 0.375 in.). The material properties of the steel, as given by the manufacturer, were a modulus of 29000 ksi and a yield strength 70 ksi. Two tensile specimens of ten inches in length were tested using a hydraulic loading frame in the Civil Engineering Structural Laboratory. One

specimen had a diameter of 0.375 in. and the other specimen had a diameter of 0.625 in. Steel plates were welded onto the bars so that they could be tested in the hydraulic frame. In order to attach a strain gage to each specimen, the ridges on the rebars needed to be smoothed out using a steel lathe. The actual diameters of the bars during testing were 0.305 in. and 0.50 in. The yield stress of the No. 3 and No. 5 bar were 75 ksi and 71 ksi, respectively. Figure 24 below shows the stress vs. strain measurements of the two bars. Figure 25 shows the two bars and how they were tested.
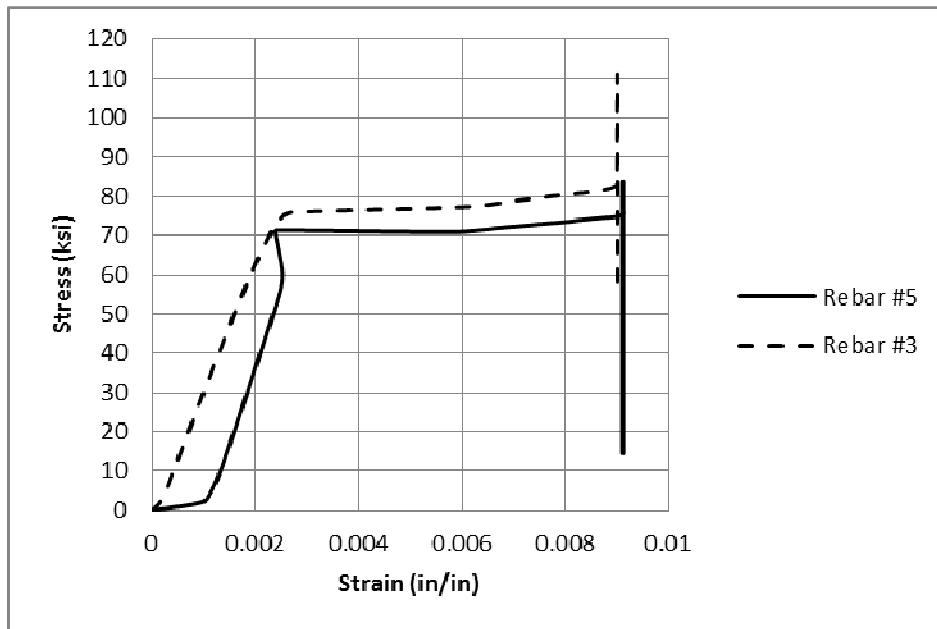

Figure 24: Stress-Strain Relationship of the Steel Rebars

Figure 25: Bars with Strain Gages attached (left) and Testing Bar in Hydraulic Frame (right)

Chapter 5 - Experimental Setup and Testing

Experimental Setup

The flexural tests were performed in the structural testing laboratory at Kansas State University. The beams were loaded in four-point bending using a spreader beam of four feet long and a 50 kip hydraulic actuator. The actuator is controlled by a servo-hydraulic system from MTS, which uses a very accurate data acquisition program and requires MTS certification in order to be properly operated.

The beams are simply supported by using plates and rollers at the supports. The supports are placed 3 in. from the ends of the beams which results in a clear span of 15.5 ft. Figure 26 shows the experimental test setup.
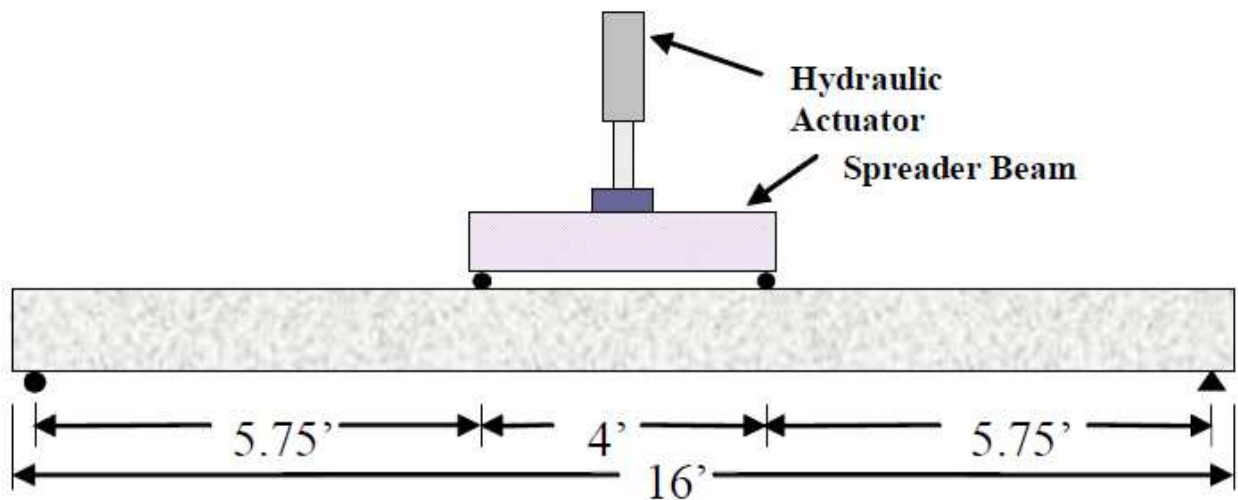

Figure 26: Experimental Test Setup

Two ten inch long linear variable differential transducer (LVDT) sensors were placed at mid-span on the top of the beams to measure deflection at mid-span. Two-120 Ω strain gages were mounted on the main flexural steel bars, with one gage on each bar at mid-span, prior to casting of the beams. Two-120 Ω resistance strain gages were also installed on the top on the beam at mid-span to obtain the maximum concrete strain while testing. Two-350 Ω gages were installed at the mid-span on the bottom of the strengthened beams on the attached GFRP to obtain the

strain in the GFRP throughout the testing procedure and most importantly at failure. Figure 27 below shows the strain gages attached to the top of the beams on the concrete and on the bottom of the beams on the GFRP. All of the instrumentation was wired into a channel data acquisition system called Megadac 200, a system developed by MTS. The data was recorded every 1.5 seconds or about every 25 lbs. Before each test, the data acquisition system was run through multiple test procedures and checks to ensure that is recording data and recording it correctly. The beams were loaded at a rate of 1000 lbs. per minute. After completing each test, the data was transferred from the data acquisition system to Microsoft Excel for analysis.

Figure 27: Strain Gages on the Concrete (left) and GFRP (right)

For the corrosion test performed on Specimen R4, a form that could fit the entire length of the beam was constructed using plywood and 2 in. x 4 in. lumber leftover from the formwork used to cast the beams, which can be seen in Figure 28 below. Then this form was lined with a thick plastic sheet folded over several times in order to retain the corrosion solution. The beam was then cracked, by being loaded 5 times up to its cracking load (Appendix B). The beam was then

placed into the form so that the solution could reach the area covered by the GFRP sheet. The corrosion solution used was a saline solution using a deicing salt and water. The solution was mixed using a concentration of 25% deicing salt by weight. Figure 29 shows the mixing of the saline solution and applying it to the beam.

Figure 28: Formwork and Plastic Lining for the Corrosion Test

Figure 29: Mixing 25% by-weight saline Solution (left) and Applying Solution to Specimen R4 (right)

Test Results

Control Beam (R1)

The first beam to be tested was the control beam, named beam R1 in this experiment. From the flexural analysis program, it was determined that the beam would have a maximum moment capacity of 35.6 kip-ft. This capacity was a result from a maximum load of 11.63 kips and a maximum deflection of 3.94 in. The beam was loaded at a rate of 1 kip per minute and the test results show that the beam achieved a maximum load of 12.24 kips, which corresponds to maximum deflection of 4.62 inches. The control beam failed in a ductile concrete crushing failure mode, which is steel yielding first followed by crushing of the concrete. Figure 30 below shows the setup of the control beam before testing was started. Figure 31 and Figure 32 show the beam after testing and the concrete crushing that occurred at failure. Figure 33 is the load vs. deflection data taken from the test.

Figure 30: Setup of Beam R1 before testing

Figure 31: Control Beam at Failure

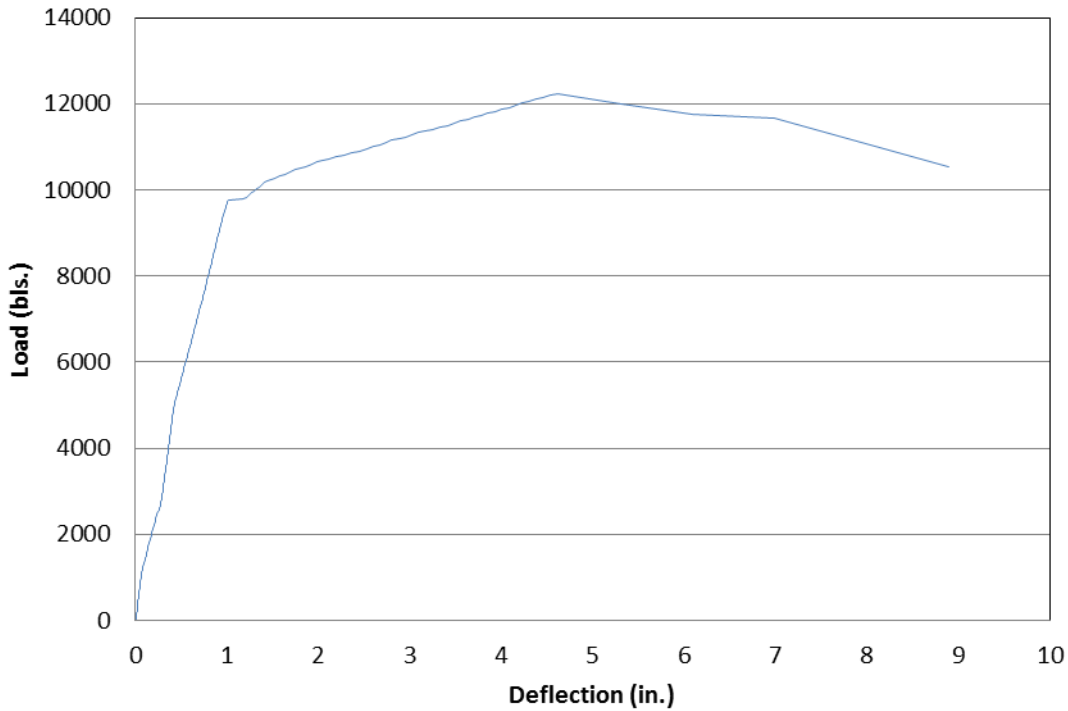**Figure 32: Concrete Crushing of Control Beam**

Figure 33: Load vs. Deflection Relationship for Control Beam

Rectangular Beam with Full Length NSM Bars and GFRP Wrapping (R2)

The next beam tested was the beam strengthened with NSM bars running the entire length of the beam along with the GFRP sheet and U-wraps. The U-wraps were used in order to prevent de-bonding of the GFRP sheet or cover delamination. This beam was predicted to have a moment capacity of 83.1 kip-ft., which corresponds to a maximum load of 28.15 kips at a maximum deflection of 2.84 inches. The beam was loaded at a rate of 1 kip per minute. The test result showed that the beam failed at a maximum load of 31.62 kips which corresponds to a maximum deflection of 3.81 inches. The beams failure mode was concrete crushing in the constant moment region. This occurred due to the beam reaching the full flexural capacity of the concrete after the steel yielded and before the GFRP ruptured. Figure 34 below shows the beam at failure and Figure 35 shows concrete crushing of the beam in the constant moment region. Figure 36 shows the test results of the load vs. deflection relationship of the beam.

41

Figure 34: Full Length NSM Beam at Failure

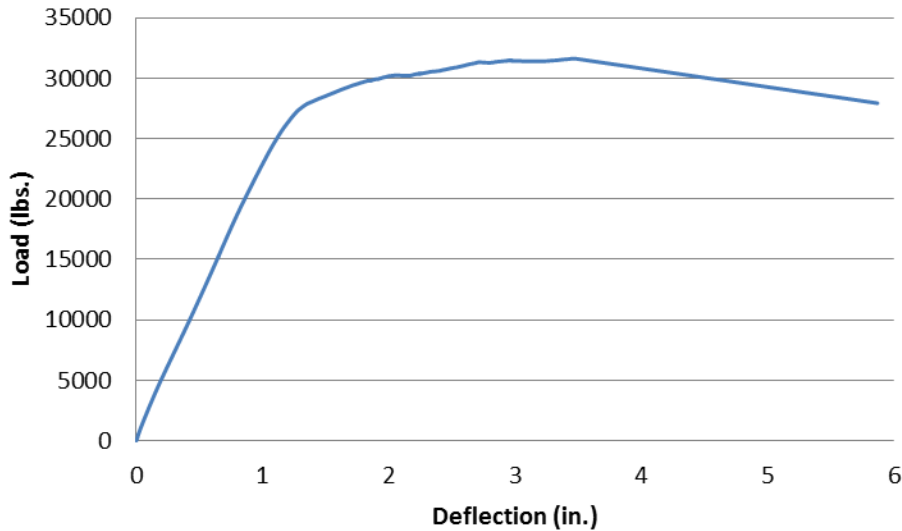**Figure 35: Concrete Crushing of Full Length NSM Beam**

Figure 36: Load vs. Deflection Relationship for the Full Length NSM Beam (R2)

Rectangular Beam with short NSM Bars and GFRP Wrapping (R3)

The third beam tested was the beam strengthened with 7 foot long NSM bars centered on the beam and the GFRP sheet and U-wraps. At the cut-off point of the NSM bars, a double layer of GFRP U-wraps were used in order to help accommodate the stress concentrations that would develop at this junction. According to theoretical analysis, the beam would have a moment capacity of 83.1 kip-ft, which corresponds to a maximum load of 28.15 kips at a maximum deflection of 2.84 inches. These are the same for Beam R2 since the analysis program could not capture the effect of the shortened NSM bars. The beam was again loaded at 1 kip per minute. The beam test results showed that the maximum load reached was 30.72 kips with a maximum deflection of 3.38 inches. The beam failed in concrete crushing mode after the beginning of yielding in the NSM bars and internal reinforcement. Figure 37 shows the beam before testing. Figure 38 shows the failure of the beam and in Figure 39 rupture of the fibers in both the sheet and U-wrap can be seen. Figure 40 shows the experimental results of the load vs. deflection.

43

Figure 37: Setup of Beam R3 before Testing

Figure 38: Failure of Beam R3

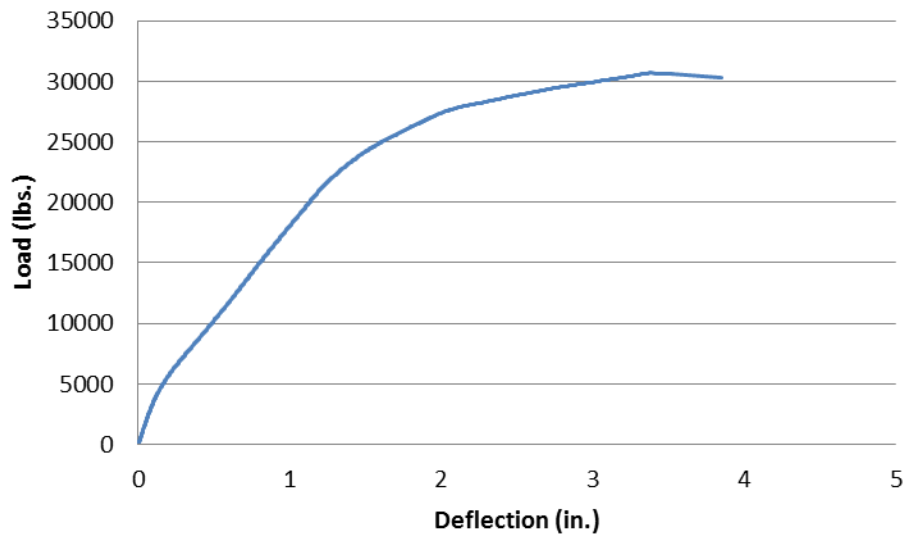**Figure 39: Rupture of GFRP sheet and U-wrap**

Figure 40: Load vs. Deflection of Beam R3

Rectangular Beam with short NSM Bars and GFRP Wrapping Exposed to Corrosion

Bath (R4)

The last beam to be experimentally tested was strengthened exactly as Specimen R3. The beam
was then loaded and un-loaded five times beyond the cracking load of the beam (up to 5 kips)

and was then submerged in a 25% by weight saline solution for six months. The load vs. time graph of the cracking procedure can be seen in Appendix B. This was done in order to test the corrosion resistance properties of the GFRP and its protection of the section and the NSM steel rebars. Therefore, after six months, the beam was tested in flexure at a rate of 1 kip per minute. The corrosion and salt residue from the corrosion test can be seen in Figure 41. The experimental results showed that the beam failed at an ultimate load of 29.8 kips which corresponded to maximum deflection of 3.16 inches. The beam failed in concrete crushing mode after the beginning of yielding in the NSM bars and internal reinforcement. Figure 42 shows the setup of the beam before testing has commenced. Figure 43 and Figure 44 shows the failed form of the beam and the failure mode, respectively. Figure 45 shows the load vs. deflection experimental results for the corrosion beam.

Figure 41: Corrosion from Salt (left) and Salt Residue (right)

Figure 42: Setup of Specimen R4 before Testing

Figure 43: Failure of Beam Specimen R4

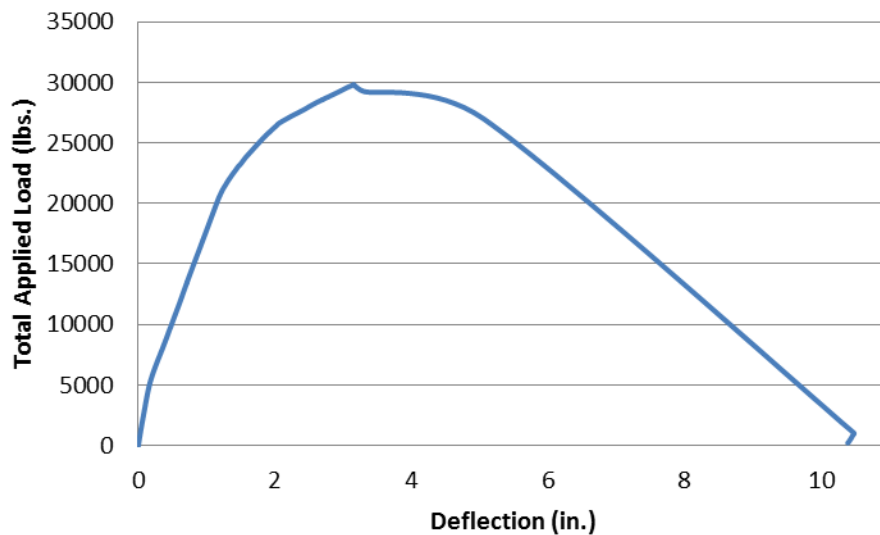**Figure 44: Crushed Concrete and Debonded U-Wrap on Specimen R4**

Figure 45: Load vs. Deflection for Specimen R4

Comparison of Specimen Behavior

As it can be seen in Figure 46, the beam strengthened with the full length NSM rebars and GFRP wrapping had the largest increase in total applied load while the beam submerged in the corrosion bath had the lowest increase in total applied load of the strengthened beams. However,

48

all three strengthened beams had very similar flexural responses. Table 3 shows a summary of the experimental results for each of the four beams.
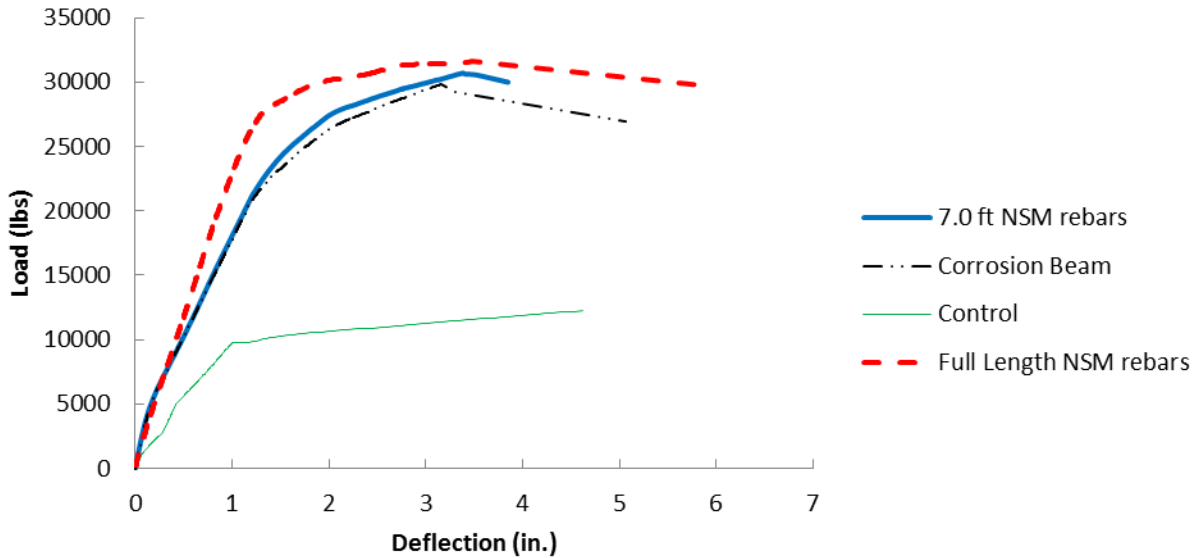

Figure 46: Comparison of Load vs. Deflection for all Beams Studied

Table 3: Summary of Experimental Results

Specimen	Ultimate Load (kips)	Deflection (in.)	Load Increase (%)	Failure Mode
Control (R1)	12.2	4.62	N/A	Concrete crushing following yielding of Steel
Full Length NSM reinf. (R2)	31.6	3.81	259.0	Concrete crushing following yielding of Steel
7 ft. NSM reinf. (R3)	30.7	3.38	251.6	Concrete crushing following yielding of Steel
Corrosion (R4)	29.8	3.16	244.3	Concrete crushing following yielding of Steel

Chapter 6 - Analysis of Results

Analysis Program

The analysis program used to design and analyze the specimens was a Microsoft Excel based program developed by Calvin Reed, a former graduate student at Kansas State University. This program gives the user the option of selecting the cross-section type, either rectangular or T-shaped, and then the appropriate dimensions are entered. The program then allows the user to select a loading type from uniform loading, three-point bending, or four-point bending. Material properties are then input such as concrete compressive strength and steel yielding strength. Different types of reinforcement can be entered such as mild steel, prestressed steel, glass bars, and/or FRP. The user can also enter the properties, size, and location of each of these different types of reinforcement. The program model predicts the flexural response of the beam by using strain compatibility and incremental deformation techniques based on the specimen geometry and material properties. The program will also allow the user to reach the code to adjust the model as needed. The program uses an iterative process to determine the moment curvature relationship. Once equilibrium is satisfied for a section, a bending moment is computed. Curvature is then determined for this moment from the strain profile. A load deflection relationship is then determined from the moment curvature relationship. An incremental analysis is performed by dividing the specimen into a large number of segments. A moment is calculated for each segment and then the curvature is determined using the moment curvature relationship. The deflection is then calculated using the moment area method.

Specimen R1

From the flexural analysis program, the control beam, specimen R1, was determined to have a moment capacity of 35.6 kip-ft. This moment capacity relates to a total applied load of 11.63 kips and a maximum deflection of 3.94 inches. The experimental test results show that specimen R1 failed at a maximum applied load of 12.24 kips which corresponds to maximum deflection of 4.62 inches. The difference in the experimental and theoretical values is 0.61 kips, which shows that the analysis program is quite accurate. The analysis program showed a failure mode of ductile concrete crushing which is exactly how the actual beam failed. The program also calculates the cracking moment to be 8.8 kip-ft or a cracking load of 3.06 kips, which is very

close to the actual cracking load of approximately 2.6 kips. Figure 47 below shows the load vs. deflection relationship for the control beam, for both theoretical and experimental results. Figures 48 and 49 show the concrete and steel strain for the control beam, respectively.
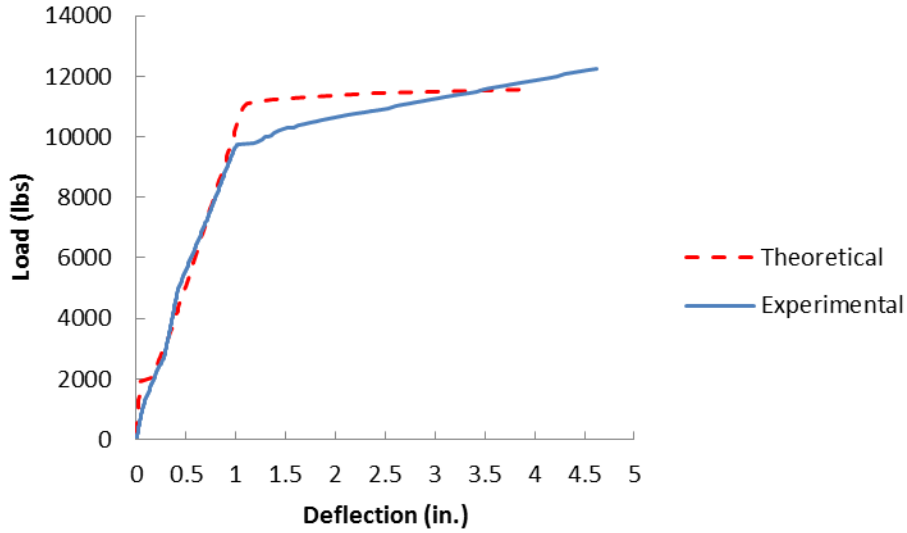

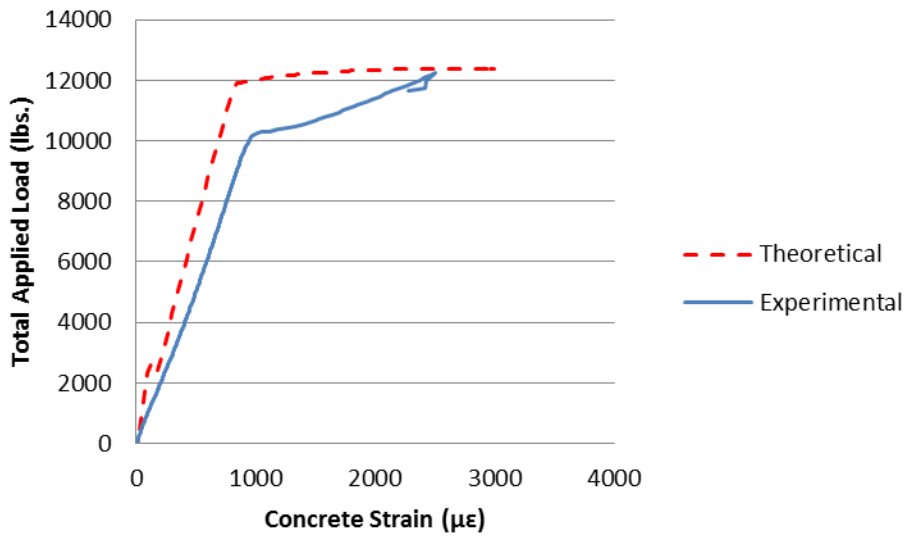**Figure 47: Load vs. Deflection of the Control Beam**

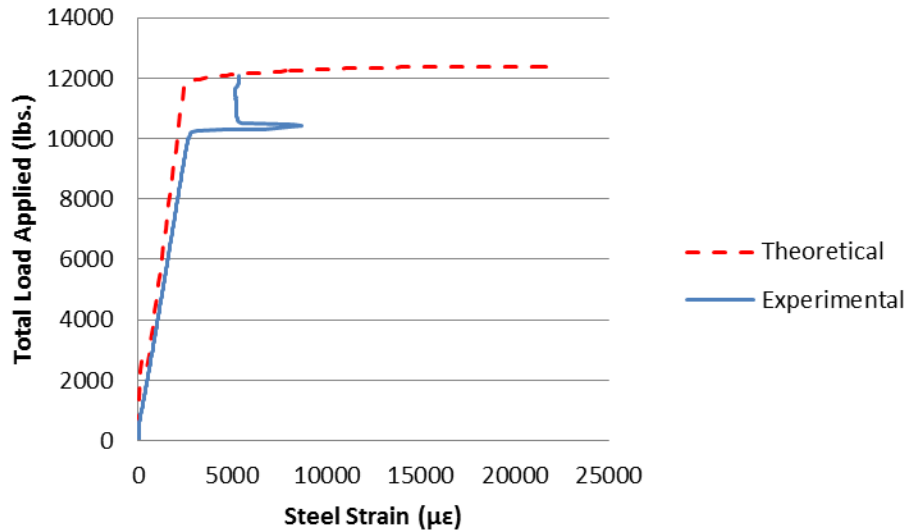**Figure 48: Load vs. Concrete Strain for the Control Beam**

Figure 49: Load vs. Steel Strain for the Control Beam

Specimen R2

The flexural analysis program predicted the beam strengthened with the full length NSM rebars and the GFRP wrapping to have a moment capacity of 83.1 kip-ft., which corresponds to a maximum load of 28.15 kips at a maximum deflection of 2.84 inches. According to the program, the failure mode would be ductile crushing of concrete. The test result showed that the beam failed at a maximum load of 31.62 kips which corresponds to a maximum deflection of 3.81 inches. The difference between the theoretical and experimental results is 3.47 kips, with the actual beam showing a slightly higher maximum deflection. The actual failure mode of the beam was ductile crushing of concrete, which was a result of the concrete reaching its full flexural capacity. Figure 50 below shows the load vs. deflection relationship for both the experimental and theoretical results for Specimen R2. Figures 51 through 53 show the load vs. strains in the concrete, tensile steel, and the GFRP sheet, respectively.
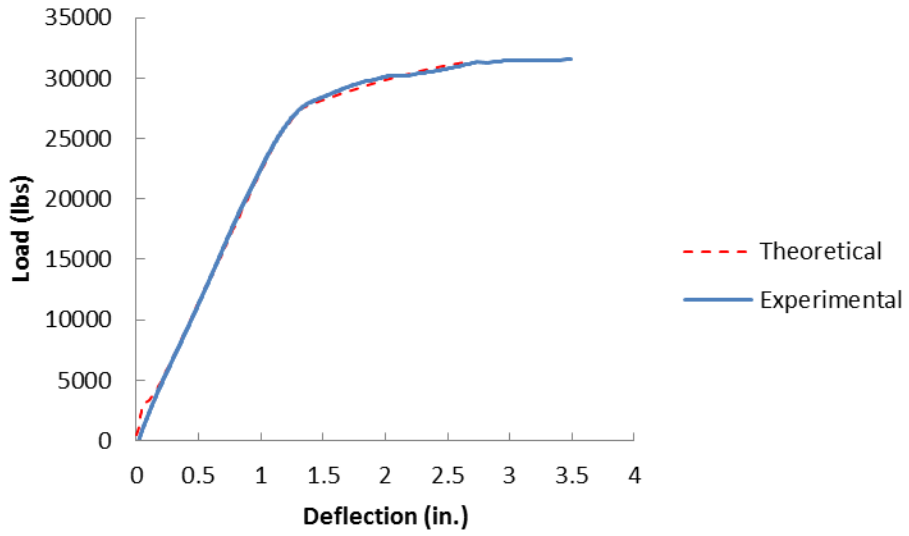
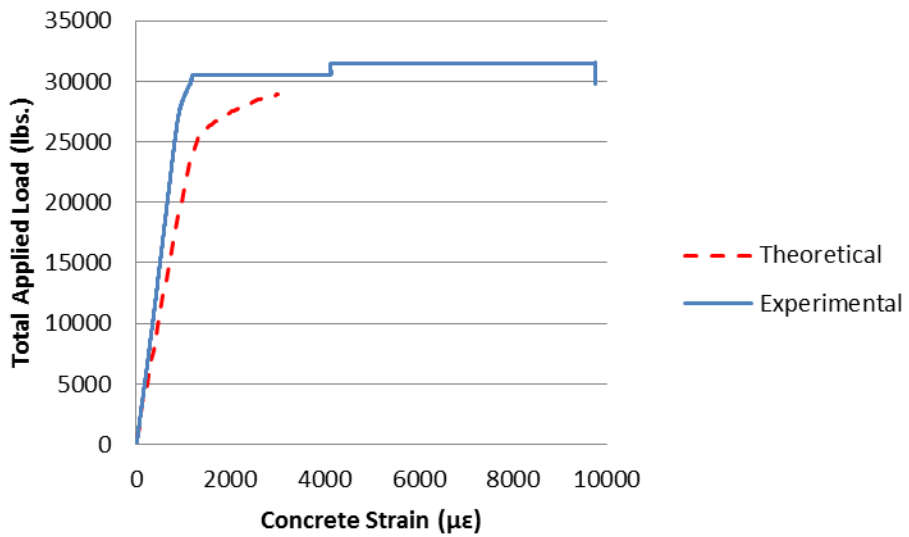**Figure 50: Load vs. Deflection for Specimen R2**
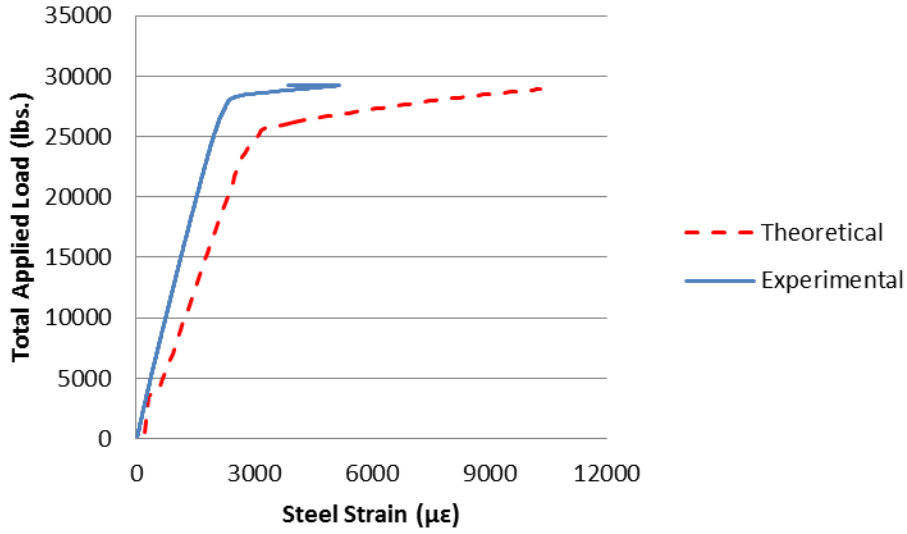

Figure 51: Load vs. Concrete Strain for Specimen R2

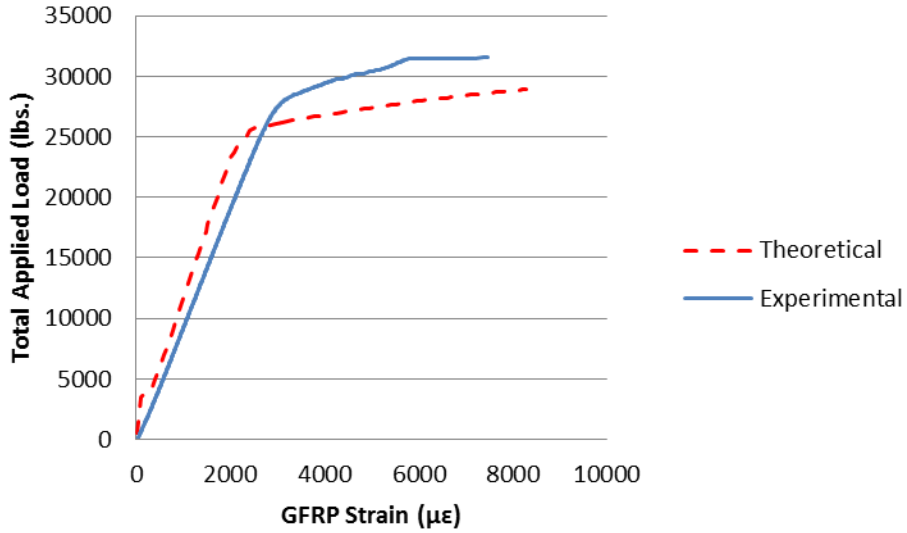**Figure 52: Load vs. Steel Strain for Specimen R2**

Figure 53: Load vs. GFRP Strain for Specimen R2

Specimen R3

The next beam to analyze is the beam strengthened with 7.0 feet long NSM steel rebars centered on the beam and a GFRP sheet with GFRP U-wraps. According to the analysis program, this beam would have a moment capacity of 83.1 kip-ft, which corresponds to a maximum load of 28.15 kips at a maximum deflection of 2.84 inches. These are the same for Beam R2 since the analysis program could not capture the effect of the shortened NSM bars. The beam test results

showed that the maximum load reached was 30.72 kips with a maximum deflection of 3.38 inches. The difference between the analysis program and the experimental results is 2.57 kips. Since the analytical program could not take into account the shortened NSM bars and the stress concentrations that would come with shortening the bars, it predicted the failure mode as ductile concrete crushing. However, due to the stress concentrations at the end of the NSM bars, the actual failure mode was a concrete crushing after yielding of internal and NSM bars. Figure 54 below shows the load vs. deflection correlation for Specimen R3. Figures 55 through 57 show the load vs. strain relationships for the concrete, steel, and GFRP sheet, respectively.
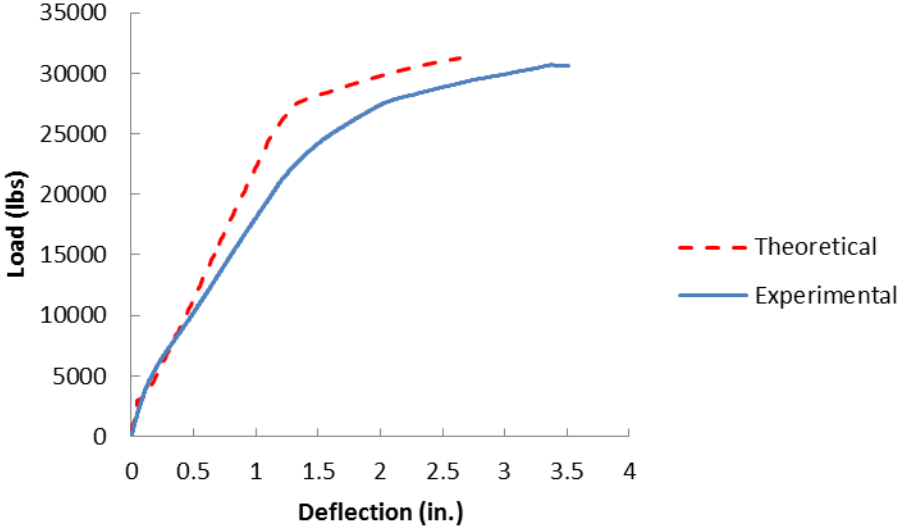
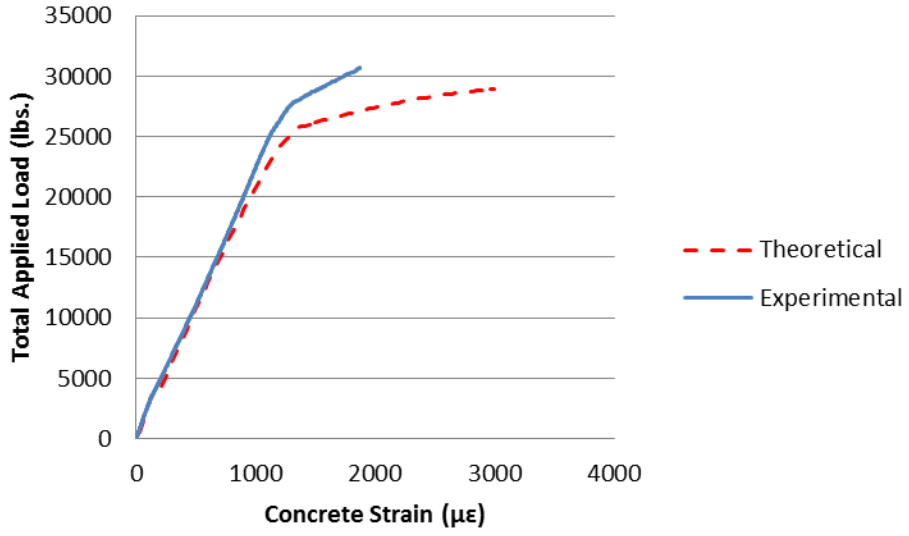**Figure 54: Load vs. Deflection for Specimen R3**

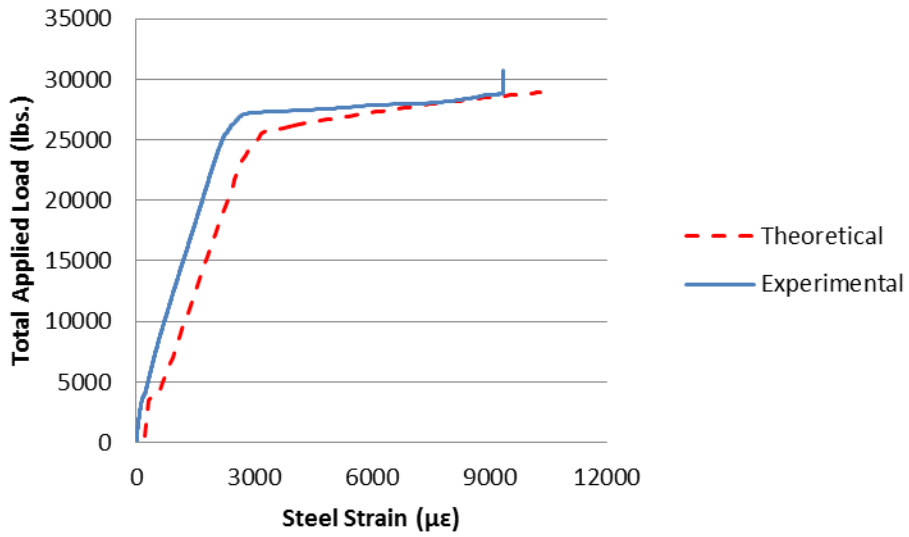**Figure 55: Load vs. Concrete Strain for Specimen R3**

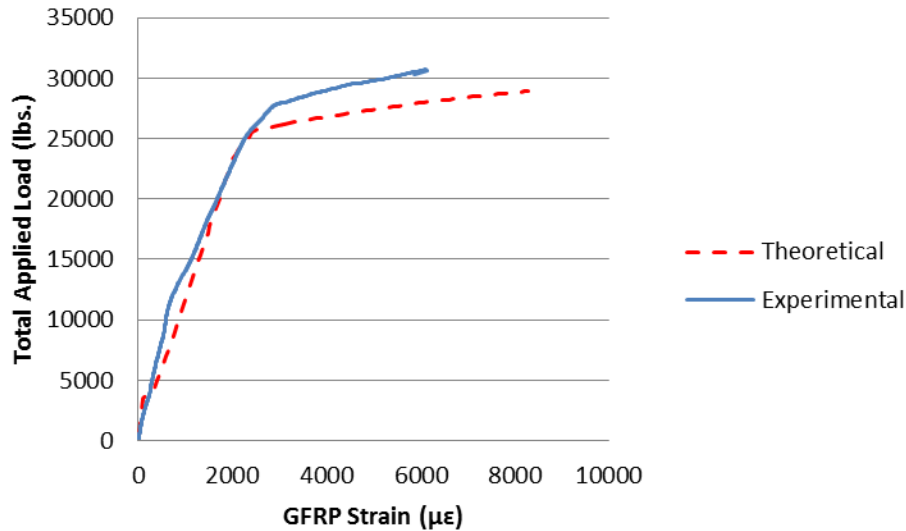**Figure 56: Load vs. Steel Strain for Specimen R3**

Figure 57: Load vs. GFRP Strain for Specimen R3

Specimen R4

The final beam to analyze is the beam strengthened exactly like Specimen R3 and then submerged in a highly concentrated saline solution for six months. The analysis program predicted this beam would have a moment capacity of 83.1 kip-ft, which corresponds to a maximum load of 28.15 kips at a maximum deflection of 2.84 inches. This prediction is exactly the same as Specimen R2 and R3 since the program cannot take into account the shortened NSM rebars and the amount of corrosion sustained from the saline solution. The experimental results showed that the beam failed at an ultimate load of 29.8 kips which corresponded to maximum deflection of 3.16 inches. The difference between the experimental and theoretical values is 1.65 kips. The difference between Specimen R3 and R4 experimental results is 0.92 kips. This result shows that the GFRP wrapping has successfully protected the section and more importantly the NSM rebars from corrosion, which was expected. Figure 58 below shows the comparison between the experimental and theoretical results for load vs. deflection. Figure 59, Figure 60, and Figure 61 show the relationships for the load vs. the strain in the concrete, tensile steel, and externally bonded GFRP, respectively.
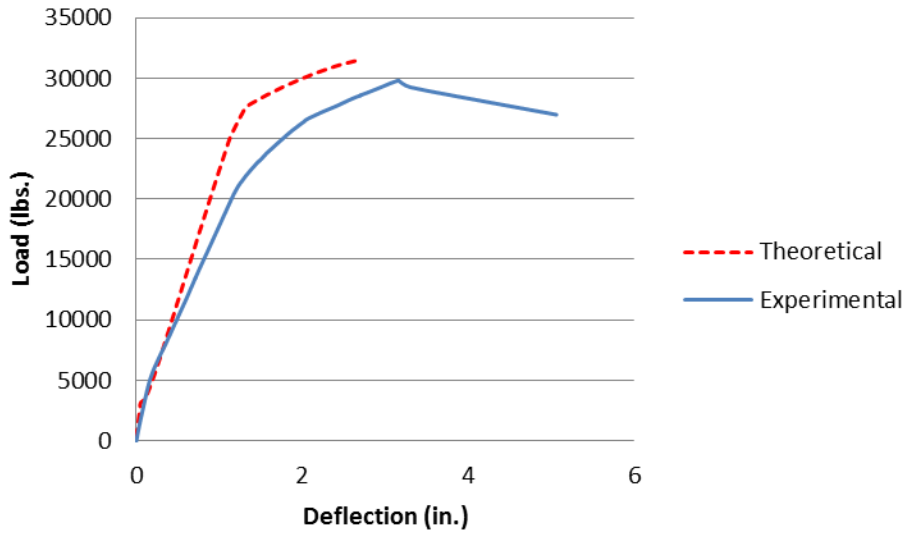
Figure 58: Load vs. Deflection for Specimen R4

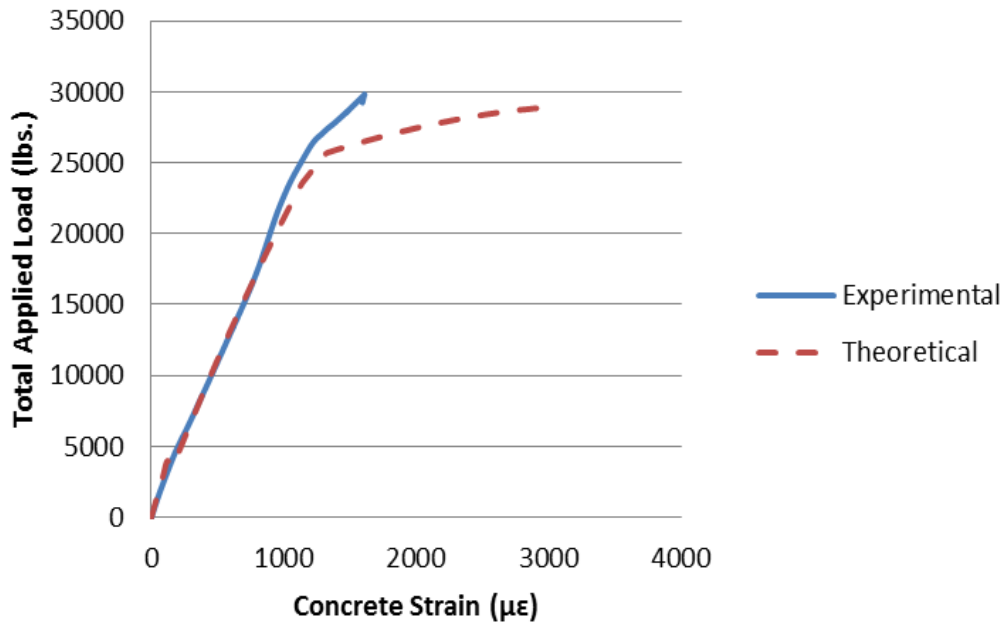**Figure 59: Load vs. Concrete Strain for Specimen R4**
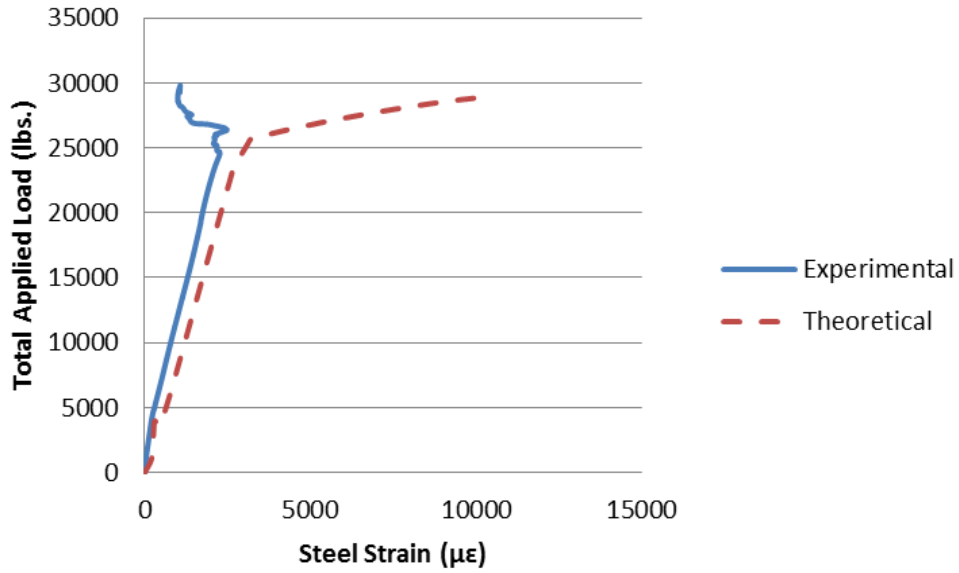
Figure 60: Load vs. Steel Strain for Specimen R4
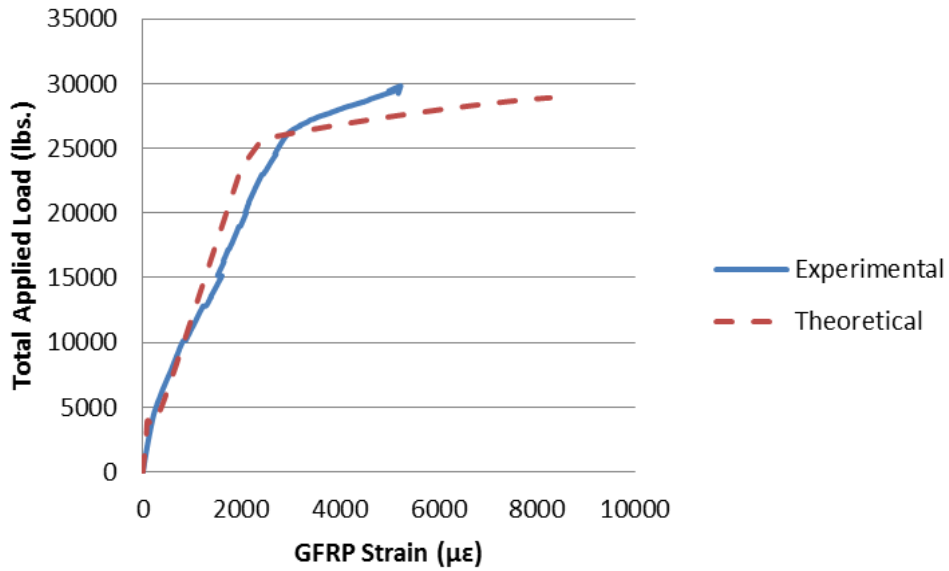
Figure 61: Load vs. GFRP Strain for Specimen R4

Comparison of Combined Strengthening Technique

By using the analytical program and the results from the flexural testing, a comparison can be made of the strength utilization of the combined strengthening technique of externally bonded

59

GFRP sheets and NSM rebars versus only using the externally bonded GFRP sheet or only the NSM rebars. Many studies have shown that using NSM bars greatly increases the flexural capacity over an externally bonded FRP system. However, from Figure 62 below, it can be seen that the total combined strength of the system is achieved through both strengthening techniques, not just NSM rebars. Since the analytical program showed good correlation to the experimental results, the load-deflection relationship of NSM rebar only and EB-GFRP sheet only should also be a good correlation, despite not having experimental data to compare.

Figure 62: Comparison of Combining Strengthening Techniques vs. using only one.

Chapter 7 - Conclusions and Recommendations

Conclusions

Throughout this study and experimental work, many conclusions can be drawn from the results. The computer program used to design and analyze the beams was very accu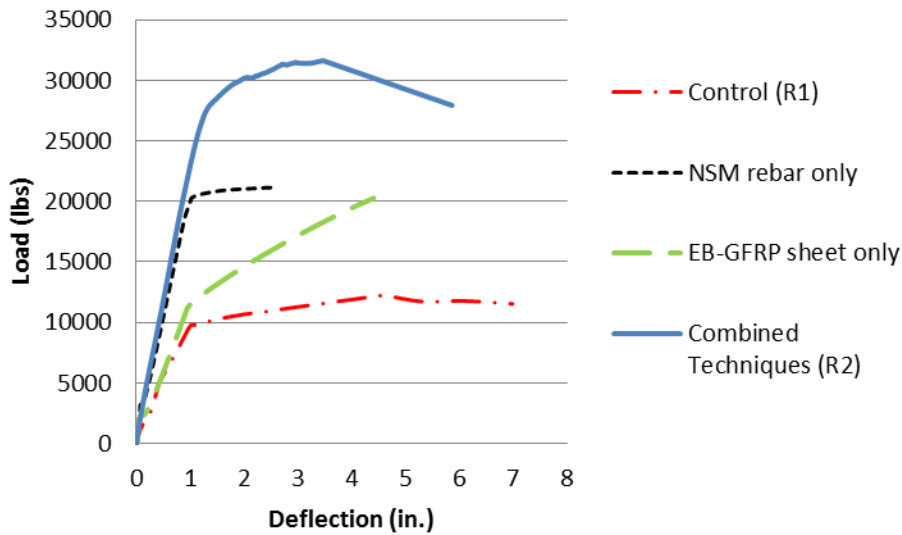rate in its predictions of the behaviors of the flexural response of the beams. Four rectangular cross section beams, one being a control beam, were tested in a four point bending test. Three of the beams were strengthened with NSM steel rebars and externally bonded GFRP fabric sheets secured with GFRP U-wraps. These beams were strengthened by preparing the surface of the beams, applying epoxy to the two NSM rebars in the grooves on the beams, and then wrapping a GFRP fabric sheet secured with GFRP U-wraps. The control beam failed at a maximum load of 12.24 kips and a maximum deflection of 4.62 inches, with a failure mode of ductile concrete crushing. The second beam was strengthened with NSM steel rebars running the entire length of the beam and wrapped with a GFRP sheet secured with GFRP U-wraps. This beam failed at an ultimate load of 31.62 kips which corresponded to a maximum deflection of 3.81 inches, with a failure mode of ductile concrete crushing. The third beam was strengthened with the exact same system as the second beam except that the NSM rebars were cut to 7.0 ft. long and centered on the mid-span of the beam. This beam failed at a maximum applied load of 30.72 kips with a maximum deflection of 3.38 inches, and a failure mode of crushing of concrete. The fourth beam was strengthened exactly as the third beam but was then pre-cracked and submerged in a 25% by-weight saline solution for six months. This was done to assess the effects of accelerated corrosion on the strengthened section. After six months, the beam was tested and failed at a maximum applied load of 29.8 kips which corresponded to maximum deflection of 3.16 inches, with a failure mode of concrete crushing.

From these results, it can be seen that the use of NSM rebars and externally bonded GFRP sheets with U-wraps can greatly increase the flexural capacity of concrete beams. The increase in strength over the control beam of the three strengthened beam ranged from 244% to 259%. It can also be shown from the small difference in maximum loads of the third (Specimen R3) and fourth (Specimen R4) beams that the use of the GFRP sheets over the NSM rebars provides good corrosion resistance. Also, the use of the combined strengthening techniques was easy to install,

61

which could result in a savings in cost due to labor and materials compared to using many layers of only FRP. The use of the GFRP can also increase the durability of the section due to its corrosion resistance properties. Since the beams strengthened with shortened NSM rebars failed at a maximum load slightly less than that of the beam strengthened with full length NSM rebars, it can be deduced that the development length of the NSM rebars was insufficient. Overall, the use of NSM rebars and externally bonded GFRP is an efficient and desirable strengthening technique due to its large increase in flexural capacity and the corrosion resistant behavior of the GFRP.

Recommendations for Future Work

This research suggests many recommendations for future work and research. The strengthening techniques worked well in the lab, a controlled environment, but on-site application would be very different. Research should be done on how moisture and temperature would affect the bond of the epoxy and resin used in the strengthening process. The corrosion test was performed over a six month period, which is a relatively short time compared to the life span of a typical concrete beam in a structure. Long term corrosion tests should be performed to obtain accurate data on the effect of corrosion on the bond of the FRP and overall strength of the beam. Also, research could be performed using a wet/dry cycles or other techniques to enhance the effectiveness of the corrosion on the element. A further study could be performed to determine the beam strength after damage sustained from a fire or an accident. Also, shear and torsion load capacity tests should be performed on the combined NSM rebar and externally bonded FRP techniques. Experimental studies could also be performed on the development length of the NSM rebars that would create an adequate strength increase comparable to using full length NSM rebar. Also, numerical and finite element models of the combined strengthening techniques could provide further insight onto the behavior of the system.

References

ACI Committee 318 (2011). Building Code Requirements for Structural Concrete and Commentary (ACI 318-11). *American Concrete Institute.*

ACI Committee 440 (2008), "Design and Construction of Externally Bonded FRP Systems for Strengthening Concrete Structures (ACI 440.2R-08)." *American Concrete Institute.*

Arduini, M. and Nanni, A., "Behavior of Precracked RC Beams Strengthened with Carbon CFRP Sheets." *Journal of Composites for Construction,* ASCE, Vol. 1, No. 2, 1997, pp. 63-70.

ASCE, "2013 Report Card for America's Infrastructure," ASCE, 2013. Available: http://www.infrastructurereportcard.org/.

Dai, J., Yokota, H., Iwanami, M., Kato, E., "Experimental Investigation of the Influence of Moisture on the Bond Behavior of FRP to Concrete Interfaces," *Journal of Composites for Construction,* Vol. 14, No. 6, 2010, pp. 834-844.

Decker, B. R., (2007) "A Method of Strengthening Monitored Deficient Bridges," Masters Thesis, Department of Civil Engineering College of Engineering, Kansas State University, Manhattan, Kansas.

Hassan, T.K., and Rizkalla, S.H., "Bond Mechanism of Near-Surface-Mounted Fiber-Reinforced Polymer Bars for Flexural Strengthening of Concrete Structures," *ACI Structural Journal,* Vol. 101, No. 6, 2004, pp. 830-839.

Kachlakev, D., and McCurry, D.D., Behavior of full-scale Reinforced Concrete Beams Retrofitted for Shear and Flexural with FRP Laminates." *Composites: Part A, Applied Science and Manufacturing,* Vol. 31, No. 6, 2000, pp. 445-452.

Nurbaiah, M.N., Hanizah, A.H., Nursafarina, A., and Nur Ashikin, M., "Flexural Behavior of RC Beams Strengthened with Externally Bonded (EB) FRP Sheets or Near Surface Mounted (NSM) FRP Rods Method," *International Conference on Science and Social Research,* December 5-7, 2010, Kuala Lumpur, Malaysia.

Rahimi, H.; Hutchinson, A., "Concrete Beams Strengthened with Externally Bonded FRP Plates," *Journal of Composites for Construction*, Vol. 5, No. 1, 2001, pp. 4456.

Rasheed, H.A., Larson, K.H., Peterman, R.J., "Analysis and Design Procedure for FRP-Strengthened Prestressed Concrete T-Girders Considering Strength and Fatigue," *Journal of Composites for Construction,"* Vol. 10, No. 5, 2006, pp. 419-432.

Soliman, S.M., El-Salakawy, E., and Benmokrane, B., "Flexural Behavior of Concrete Beams strengthened with Near Surface Mounted Fibre Reinforced Polymer Bars," *Canadian Journal of Civil Engineering,* No. 37, 2010, pp. 1371-1382.

Soudki, K.A., Sherwood, T., and Masoud, S., "FRP Repair of Corrosion-Damaged Reinforced Concrete Beams," *American Concrete Institute Fall Convention,* Toronto, October, 2000.

Soudki, K., El-Salakawy, E., and Craig, B., "Behavior of CFRP Strengthened Reinforced Concrete Beams in Corrosive Environment," *Journal of Composites for Construction,* Vol. 11, No. 3, 2007, pp. 291-298.

Sun, Z.Y., Wu, G., Wu, Z.S., and Luo, Y.B., "Flexural Strengthening of Concrete Beams with Near-Surface Mounted Steel-Fiber-Reinforced Polymer Composite Bars," *Journal of Reinforced Plastics and Composites,* Vol. 30, No. 18, 2011, pp. 1529-1537.

"V-Wrap Composite Strengthening System," PART I: Surface Repair & Preparation. S.l.: Structural Technologies, April 26, 2012.

"V-Wrap Composite Strengthening System, PART II: Installation of V-Wrap Sheet. S.l.: Structural Technologies, April 26, 2012.

Wang, C., Shih, C., Hong, S., Hwang, W., "Rehabilitation of Cracked and Corroded Reinforced Concrete Beams with Fiber-Reinforced Plastic Patches," *Journal of Composites for Construction,* Vol. 8, No. 3, 2004, pp. 219-228.

Zhang, H., Wang, L., Liu, G., "Flexural Behavior and Ductility of Concrete Beams Strengthened with Near-Surface-Mounted GFRP Bars," *Journal of Composites for Construction,* Vol 163-167, No. 4, 2011, pp. 3610-3614.

Appendix A - GFRP Properties

The manufacturer cured laminate properties are provided by the producer (Table A-1). However, the cured laminates GFRP were tested according to ASTM D3039. Figure A-1 shows the stress-strain relationship of the tensile test of GFRP composite laminates that was performed at Kansas State Mechanical Engineering lab. The actual measurements are shown in Table A-2 and the results are shown in Table A-3.

Table A-1: Manufacturer Cured Laminate Properties of GFRP

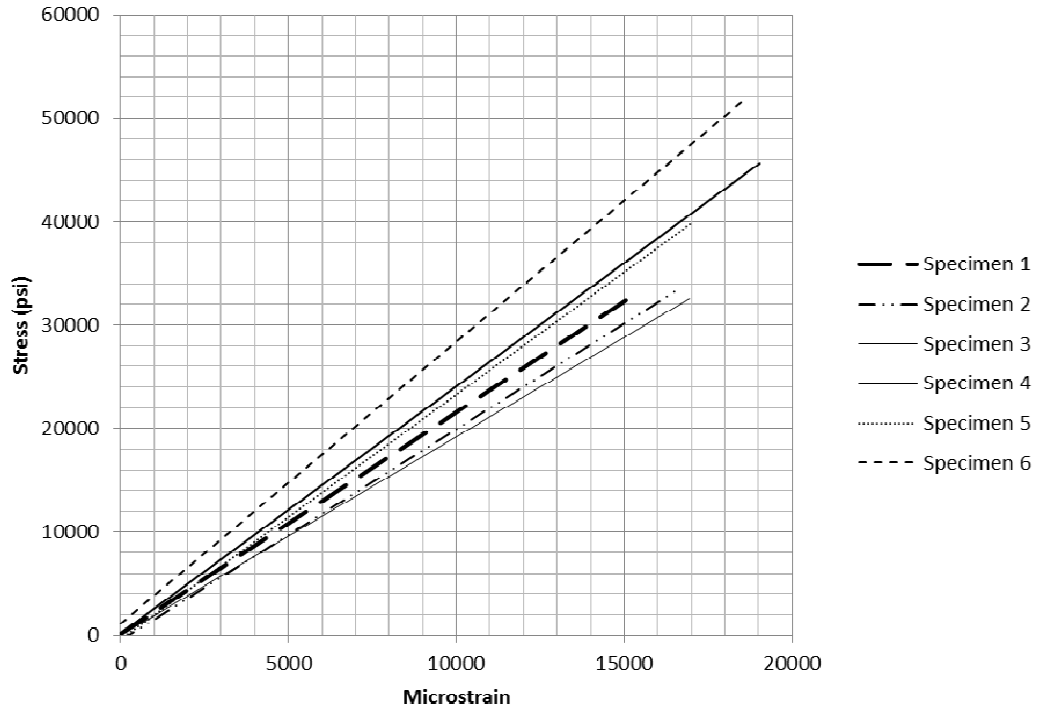|	Tensile Strength:	Modulus of Elasticity	Elongation at Break	Thickness	Strength per Inch Width
Average Value	83,400 psi	3.79×10^6 psi	2.2%	0.05 in	4,170 lbs/layer
Design Value	66,720 psi	3.03×10^6 psi	1.76%	0.05 in	2,660 lbs/layer

Figure A-1: Stress vs. Strain of GFRP Composite Laminates

Table A-2: Dimensions of GFRP Specimens and Failure Load

Coupon Specimen	Layers	Thickness 1 (in.)	Thickness 2 (in.)	Average Thickness (in.)	Width (in.)	Failure Load (Ib)	Cross Sectional Area (in^2)
1	1	0.096	0.102	0.0990	1.0	3300	0.099
2	1	0.105	0.102	0.1035	1.0	3800	0.1035
3	1	0.112	0.110	0.1110	1.0	3550	0.111
4	2	0.162	0.170	0.1660	1.0	7450	0.166
5	2	0.141	0.143	0.1420	1.0	5465	0.142
6	2	0.152	0.151	0.1515	1.0	7600	0.1515

Table A-3: Results of Tensile Test for GFRP Coupons

Specimen	Width	Average Thickness	Ultimate Strength (ksi)	Modulus(ksi)	Ultimate Strain (με)
GFRP-1	1.00	0.099	32.7	2173	15065
GFRP-2	1.00	0.103	32.7	1971	16598
GFRP-3	1.00	0.111	31.9	1886	16936
GFRP-4	1.00	0.166	44.5	2026	21954
GFRP-5	1.00	0.142	38.5	2265	16987
GFRP-6	1.00	0.152	50.2	2688	18675
Average GFRP	-	-	38.4	2168	17702

Appendix B - Cyclic Load Procedure to Crack Specimen R4 Prior to Corrosion Exposure

Figure B-1 below shows the cyclic load used to crack the specimen used for the corrosion test (Specimen R4), in order to simulate a beam in-service that is submitted to a corrosive environment.
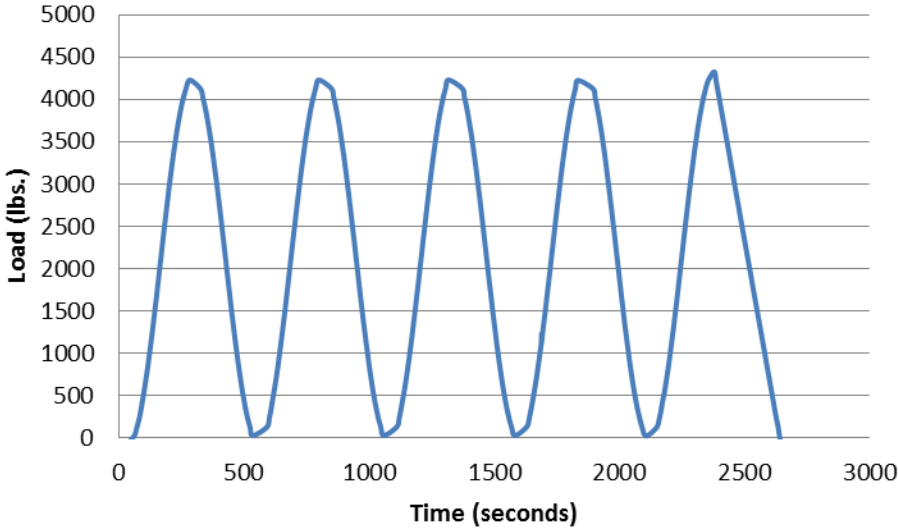

Figure B-1: Load vs. Time used to Crack Speciment R4